Responses of the Mediterranean seagrass *Cymodocea nodosa* to combined temperature and salinity stress at the ionomic, transcriptomic, ultrastructural and photosynthetic levels

Soultana Tsioli [a,b], Maria Koutalianou [a], Georgios A. Gkafas [c], Athanasios Exadactylos [c], Vasilis Papathanasiou [b], Christos I. Katsaros [a], Sotiris Orfanidis [b], Frithjof C. Küpper [d,e,f,*]

[a] *Department of Biology, National and Kapodistrian University of Athens, Panepistimiopolis, Athens, 157 84, Greece*
[b] *Benthic Ecology & Technology Laboratory, Fisheries Research Institute (Hellenic Agricultural Organization-DEMETER), 64007, Nea Peramos, Kavala, Greece*
[c] *Department of Ichthyology and Aquatic Environment, School of Agricultural Sciences, University of Thessaly, Fytokou str., 384 46, Volos, Greece*
[d] *School of Biological Sciences, Cruickshank Bldg., University of Aberdeen, St. Machar Drive, Aberdeen AB24 3UU, Scotland, UK*
[e] *Marine Biodiversity Centre, Department of Chemistry, University of Aberdeen, Aberdeen, AB24 3UE, Scotland, UK*
[f] *Department of Chemistry and Biochemistry, San Diego State University, CA, 92182-1030, USA*

ARTICLE INFO

ABSTRACT

The Little Neptune grass *Cymodocea nodosa* is a key seagrass species in the Mediterranean Sea, forming extensive and patchy meadows in shallow coastal and transitional ecosystems. In such habitats, high temperatures and salinities, separately and in combination, can be significant stressors in the context of climate change, particularly during heatwave events, and seawater desalination plant effluents.

Despite well-documented negative, macroscopic effects, the underlying cellular and molecular processes of the combined effects of increasing temperature and salinities have remained largely elusive in *C. nodosa* – which are addressed by the present study. High salinity and high temperature, alone and in combination, affected ion equilibrium in the plant cells. Non-synonymous mutations marked the transcriptomic response to salinity and temperature stress at loci related to osmotic stress. Cell structure, especially the nucleus, chloroplasts, mitochondria and organization of the MT cytoskeleton, was also altered. Both temperature and salinity stress negatively affected photosynthetic activity as evidenced by $\Delta F/Fm'$, following an antagonistic interaction type.

Overall, this study showed that all biological levels investigated were strongly affected by temperature and salinity stress, however, with the latter having more severe effects. The results have implications for the operation of desalination plants and for assessing the impacts of marine heat waves.

1. Introduction

Seagrasses are ecosystem engineers in seabed communities in many tropical to temperate seas of the world (Waycott et al., 2006). They play major roles as shelters, nurseries (Ermgassen et al., 2016) and for benthic carbon sequestration (Trevathan-Tackett et al., 2015). Seagrasses are polyphyletic members of the Alismatales, whose evolutionary ancestors have returned to the sea (Waycott et al., 2006). In the Mediterranean, 4 seagrass species are native: *Posidonia oceanica* (L.) Delile, *Cymodocea nodosa* (Ucria) Ascherson, *Zostera marina* L. and *Z. noltei* Hornemann. Among these, the 2 most important structuring species of seagrass communities are *P. oceanica* and *C. nodosa.*

Cymodocea nodosa (Fig. 1) is considered a pioneering species and thought to be more tolerant to environmental fluctuations than *P. oceanica* (Den-Hartog, 1970; Pergent et al., 2014). A succession of *C. nodosa* communities has been shown to often precede *P. oceanica* climax communities (Cancemi et al., 2002). A recent study explored the population genetics of *C. nodosa* in Greek waters (Gkafas et al., 2016). In the South-eastern Mediterranean, the tropical species *Halophila stipulacea* and *H. decipiens* are recent arrivals through the Suez Canal (Gerakaris et al., 2020; Sghaier et al., 2011). Mediterranean seagrasses have also been used for assessing benthic marine environmental quality (Orfanidis et al., 2001, 2010; Papathanasiou and Orfanidis, 2018).

An important milestone was the recent sequencing of the first

---

Fig. 1. *Cymodocea nodosa* in its natural habitat at ca. 3 m depth off the Dodecanese island of Halki, Greece, on June 17, 2021.

genome of a seagrass, *Z. marina* (Olsen et al., 2016), which revealed that near-permanent life underwater came with the loss of key terrestrial angiosperm innovations. In particular, all stomatal genes were lost, but also genes involved in terpenoid synthesis and ethylene signalling as well as genes for UV protection and phytochromes for far-red sensing. Conversely, newly acquired features and regain of functions include full salinity tolerance, synthesis of polyanionic, low-methylated pectins and sulphated galactans (the latter are common in all macroalgae) besides all polysaccharides of land plants, and also O_2/CO_2 exchange through leaf epidermal cells. In the same context, other –omics studies are currently contributing to a better understanding of the fundamentals of seagrass biology. Golicz et al. (2015) conducted a genome-wide survey in the Australian seagrass *Zostera muelleri*, revealing loss of genes related to ethylene signalling, presumably in adaptation to a permanently submerged life mode.

Temperature and salinity are considered key stressors for seagrasses, both relevant in an indirect context such as global climate change (Küpper and Kamenos, 2018), but also more directly, such as saline brine discharges from desalination plants and industry. Shallow coastal ecosystems are particularly vulnerable to global warming because increased temperatures may interact in an additive (joint effect is the sum of the effects of both stressors in isolation), synergistic (the combined effect is greater than the additive effects) or antagonistic (the combined effect is lower than the additive effects) way with other physical and anthropogenic stressors (Humanes et al., 2016; Koch et al., 2007; Ontoria et al., 2020; York et al., 2013). Especially extreme events such as heatwaves where temperatures increase well above background levels for days (Hobday et al., 2016) may also increase seawater evaporation and, therefore, the salinity of partly enclosed, shallow bays or coastal lagoons. For example, although climate change simulations show a long-term decrease in salinity in the hypersaline lagoon Mar Menor, Spain, due to seawater level rise, they also show increasing temperatures by several degrees, and heat wave events may increase background salinity values of the lagoon with predictions ranging from 38.1 to 51‰ (De Pascalis et al., 2012). Also low salinity can constitute a formidable stress for seagrass physiology, e.g. during flood events and near river estuaries (Lamit and Tanaka, 2021). These changes are especially detrimental for the typical inhabitants of those ecosystems, including seagrasses (Marbà and Duarte, 2010), and as ecosystem engineers, it will have cascading effects on ecosystem functions and biodiversity (Hoegh-Guldberg et al., 2007; Smale et al., 2019; Wernberg et al., 2012). Therefore, predicting how specific stressors interact with seagrasses is essential in their conservation and management (Galli et al., 2017; He and Silliman, 2019; Stockbridge et al., 2020). Warm and highly saline brine discharges from seawater

desalination plants in the Mediterranean (Fernandez-Torquemada and Sanchez-Lizaso, 2005; Garrote-Moreno et al., 2014; Latorre, 2005; Xevgenos et al., 2021) are getting more and more common on warm-temperate, often arid coasts around the world. The discharged brine typically has around 44–90‰, depending on the type of plant and desalination technology used (Fernandez-Torquemada and Sanchez-Lizaso, 2011 and references therein) – e.g., for a desalination plant near Alicante, Spain, a brine salinity of 68‰ was reported (Garrote-Moreno et al., 2014).

Seagrasses often experience salinity and temperature stresses simultaneously, affecting multiple biological levels, from molecular to sub-cellular and physiological, decreasing the species growth and fitness (Pandey et al., 2017). For example, at the transcriptomic level, the expression of genes encoding photosynthetic proteins (including PSII reaction centre proteins) of *C. nodosa* was significantly downregulated in the first 24 h of heat stress (Malandrakis et al., 2017a). However, studies on the effect of different abiotic stress parameters in seagrasses especially in *C. nodosa*, are limited.

There are few publications dealing with the effects of increased temperatures and salinity on the cell structure and MT organization of different seagrass species (Benjamin et al., 1999; Iyer and Barnabas, 1993; Jagels and Barnabas, 1989; Koutalianou et al., 2016; Serra et al., 2013; York et al., 2013). Short term experiments at increased temperature conditions caused severe disturbance in cell structure and cell division (Koutalianou et al., 2016). However, there is limited information on the effects of salinity stress on the cell ultrastructure of seagrasses – a single study by Jagels and Barnabas (1989) reports that high salinity caused highly vacuolated cells with few chloroplasts and mitochondria.

High temperatures usually inhibit PSII activity through oxidative damage to PSII proteins; D1 protein seems to be damaged by lipid peroxidation occurring near PSII (Yamamoto, 2016). In addition, salt stress leads to chlorophyll content reduction by inhibiting chlorophyll synthesis or accelerating degradation (Zhao et al., 2007). Therefore, PSII is considered an essential sensitive target to environmental stresses (Maxwell and Johnson, 2000).

Following our recent studies of transcriptomic responses (Malandrakis et al., 2017a) as well as photosynthesis (Tsioli et al., 2019) in *C. nodosa* under extreme temperature, salinity and their combination, but also the epiphytes of the leaves of this seagrass species (Tsioli et al., 2021), this study was conducted in order to unravel key ecophysiological, cellular and molecular features of the response of the Mediterranean seagrass *C. nodosa* to salinity and temperature stress, using a combination of transcriptomics, ionomics, physiological measurements, immunofluorescence and electron microscopy. Significantly, to the best of our knowledge, this is the first study applying ionomics (Salt et al., 2008) to a seagrass.

2. Materials and methods

2.1. Plant material

Intact shoots of *C. nodosa* were collected using scuba diving from 0.8 m to 3 m depth at Cape Vrasidas (Gulf of Kavala; 40°49′37.53″N, 24°19′8.78″E), and were transported in plastic containers containing seawater to the laboratory of the Benthic Ecology & Technology Laboratory for the medium-term experiments (FRI – Kavala). Similarly, for the short-term experiments, intact shoots were collected from the western coast of South Evoikos Gulf (38°24′ N, 23° 40′E), Greece and were transported in plastic containers to the laboratory of the Department of Biology (University of Athens).

After being transported to the laboratory for medium-term experiments, shoots were cleaned and then left to acclimatize for 10 days in 5 l well-aerated aquaria at 21–22 °C, 60 μmol photons m^{-2} s^{-1}, 14 h light per day. The aquaria contained 4 l artificial seawater medium (33.5‰ salinity, 0.3 μM NO$_3^-$, and 0.02 μM PO$_4^{3-}$) produced by Münster™ Sea

Salt (Meersalz) diluted in resin-filtered tap water (<15 µS/cm). For the photosynthesis and transcriptomics experiments entire leaves or parts of the leaves were used, respectively, while for the ultrastructure experiments, the material was taken from the meristematic region of either the smallest juvenile leaf or the second smallest juvenile leaf. The transcriptomics material was transported in silica-gel filled plastic containers to the Hydrobiology-Ichthyology Lab of DIAE (University of Thessaly), and the material for the ultrastructure analysis was transported in synthetic sea water (below) with 4% paraformaldehyde of the first stage of fixation of each experiment to the laboratory of the Department of Biology (University of Athens).

For short-term experiments, the shoots were cleaned of debris and placed in artificial seawater (deionized H_2O with 3.1% Red Sea Salt™; Red Sea, Eilat, Israel). The cultures were grown under 88 µmol m^{-2} s^{-1} of cool white fluorescent lighting on a 14:10 light/dark cycle at room temperature (21 °C). For all ionomics experiments, the material was taken from the meristematic region of either the smallest juvenile leaf or the second smallest juvenile leaf. Small pieces of 0.5 cm height × 0.3–0.7 cm length were cut.

2.2. Treatments and response variables

2.2.1. Short-term heat and salinity stress experiments

The short-term salinity experiments were performed by using a portable conductivity meter for adjusting salinities (WTW, Weilheim, Germany) and the heat stress experiments using a thermal incubator (OilBath ONE; Memmert, Schwabach, Germany). The salinity experiments were conducted in a constant temperature chamber (21–22 °C) and the heat stress experiments at a constant salinity level (35‰), respectively. Three to six leaves were assigned per treatment and light conditions were 88 µmol photons m^{-2} s^{-1}, 14:10 light per day.

The upper thermal tolerance experiments for ionomic analysis were performed as described above, lasting from half to 6 h treatment at 34, 36, 38 and 40 °C (Suppl. Table S1). Likewise, upper salinity tolerance experiments were performed as described above, incubating *Cymodocea* for 1, 2, 4 and 6 h of treatment at 20, 35, 50, 65 and 70‰ salinity and 60–90 µmol photons m^{-2} s^{-1}, 14 h light per day at salinity 35, at a temperature of 21–22 °C respectively. Leaves were rinsed with deionized water and placed into an oven at 92 °C to dry for more than 24 h. After cooling, 3 representative samples from each treatment were weighed.

The samples were digested in Pyrex™ vials using 1.50 ml HNO$_3$ (Fisher TraceMetal grade) at 118 °C for 4 h. Then each sample was dissolved in 16.0 ml with 18 MΩ of water and analyzed using a Thermo Elemental PQ ExCell ICP-MS machine using a glass conical nebulizer that has the ability to pour 1 ml every minute. The samples were tested with 2X repeatability using ICP-MS, using both hot and cold plasma to accurately measure all 18 elements of our interest. Internal specimens of Beryllium, Gallium and Niobium (EM Science) were used by the National Institute of Standards and Technology traceable calibration standards (ULTRA Scientific, Kingstown, RI, USA). Single element standard stock solutions for the calibration procedure and for spiking yeast growth media were obtained from ULTRA Scientific.

The ICP-MS analysis was performed on lithium, sodium, magnesium, phosphorus, potassium, calcium, chromium, manganese, iron, cobalt, nickel, copper, zinc, arsenic, selenium, molybdenum, cadmium, lead and boron. The most reliable and accurate data are those for potassium, calcium, manganese, copper, zinc, molybdenum and cadmium. Exact quantitative determination of elements was conducted according to the method of Salt and co-workers (Danku et al., 2009; Salt et al., 2008) with the calculation based on Lahner et al. (2003) - and after removing the elements contained in the artificial sea water used in the short-term experiments. The choice of elements was determined both by what are the routine elements analyzed in relatively closely related higher plants and by the analytical capabilities available (Salt et al., 2008).

2.2.2. Medium-term heat and salinity, and their interaction stress experiments

The upper thermal tolerance limits were determined after 20 days of treatment at 32, 34, 35, and 36 °C, respectively. These experiments were performed in 1 L glass vessels holding one plant each, submerged in Haake™ (ThermoFisher Scientific, Waltham MA, USA) cryo-thermostats (±0.2 °C). Six replicates were assigned per treatment and light conditions were 60–90 µmol photons m^{-2} s^{-1}, 14 h light per day. The aerated medium was the same as the one used during acclimation and was changed every other day.

The optimum, upper and lower salinity limits were determined after 20 days by applying salinities of 20, 30, 35, 50, 55 and 60‰, respectively, measured using a portable conductivity meter (WTW, Weilheim, Germany). The salinity experiments were conducted in a constant temperature chamber (21–22 °C), using 2 l plastic aquaria. Six replicates were assigned per treatment and light conditions were 60–90 µmol photons m^{-2} s^{-1}, 14 h light per day. The aerated medium was the same as the one used during acclimation (except for the salinity) and was changed every other day. Each plastic aquarium was filled with 1 l of medium and contained one shoot.

To study the interaction between upper temperature and salinity stresses on *C. nodosa*, the following treatments were used: a) Control group - C (salinity 35‰, temperature 22 °C), b) Heat stress group - HS (salinity 35‰, temp. 34 °C), c) Osmotic stress group – OS (salinity 50‰, temp. 22 °C), d) High temperature and salinity – HOS (salinity 50‰, temp. 34 °C). We chose a salinity of 35‰ and temperature of 22 °C as a control to deliver typical Mediterranean Sea early spring conditions. We chose a salinity of 50‰ and temperature of 34 °C to lead the plants to the stage of resistance response phase (Lichtenthaler, 1996b) based on the study of Tsioli et al. (2019). Due to space limitations in the laboratory, the experiments were run twice consecutively. A sampling of six shoots (30 in total) was conducted at days 1, 3, 5, 10 and 20 for further analysis. The aerated medium was the same as the one used during acclimation, except for the salinity treatments, and was changed every other day. The light conditions were 60–90 µmol photons m^{-2} s^{-1}, 14 h light per day.

For preparing material for cytological studies, incubations at temperatures of either 32, 34 or 36 °C for 20 days, salinity of 50‰ for 20 days or a combination of a temperature of 34 °C with 50‰ salinity for 20 days, respectively, were applied. Tubulin immunofluorescence was applied on either the smallest juvenile leaf or the meristematic region or the next smallest juvenile leaf of each collected shoot. In both cases small leaf pieces were used, following the protocol of Katsaros and Galatis (1992) with a modified enzyme solution for the softening of the cell walls which contained 2.5% (w/v) cellulase Onozuka (Yakult Honsha Co., Tokyo, Japan), 2% (w/v) macerozyme Onozuka (Yakult), 1% (w/v) driselase from Basidiomycetes sp. (Sigma, St. Louis, MO, USA), 1% (v/v) β-glucuronidase Type HP-2, from *Helix pomatia* (Sigma) in PEM buffer (0.1 mM Pipes, 2 mM EGTA, 1 mM magnesium sulfate), pH 5.6, for 80 min. Following rinsing with PEM, the leaves were squashed on coverslips coated with 1 mg/mL poly-L-lysine (Sigma) and left to allow the separated cells to dry. For the tubulin labelling both anti-a-tubulin (YOL1/34, AbD Serotec, Kidlington, UK) and FITC-anti-rat secondary antibody (Sigma) diluted at 1:40 were used. DNA was counterstained with 10 µg/mL Hoechst 33258 (Sigma) and the cells or small leaf pieces were finally mounted in an anti-fade solution of 1.6 mg.ml-1 p-phenylen-diamine (Sigma) diluted in a solution containing 2:1 glycerol:PBS. The samples were examined with a Zeiss Axioplan microscope equipped with an ultraviolet source, proper filters and a Zeiss Axiocam MRc5 digital camera.

For transmission electron microscopy (TEM) study, the protocol reported by Katsaros et al. (1983) was followed. Thin sections were examined with a Philips 300 electron microscope (Department of Biology, National and Kapodistrian University of Athens) and a JEOL 100S TEM (Faculty of Crop Science of the Agricultural University of Athens (AUA)).

Studied samples (3 plants/treatment) were obtained after 24 h for

transcriptome analysis with RNA-seq. Leaf pieces (10 mg) were immersed in RNAlater® (Life Sciences, USA) and stored at −20 °C until downstream analysis. Transcriptomics sequencing was conducted as described previously (Malandrakis et al., 2017a) using the 12 samples of the stress experiments described above (after 24 h incubation). Twelve cDNA libraries (4 treatments x 3 samples) were sequenced in an Illumina HiSeq 2500 System and yielded 176 Gbp of data. Raw RNA reads were mapped against *C. nodosa* transcriptome (Malandrakis et al., 2017a) using STAR software (Dobin et al., 2013) and SNP variants were called through GATK software following best-practices workflow (McKenna et al., 2010). The dataset was thoroughly filtered and the processed libraries were pooled. This pipeline analysis of this dataset has been published previously (Malandrakis et al., 2017a). In the present manuscript, we performed a more appropriate alignment of the raw fastq files to the *Zostera marina* reference genome, using high-profile bioinformatic tools relevant to RNA-seq.

The software STAR was used for mapping RNA reads to a reference (Dobin and Gingeras, 2015) because of its increased sensitivity compared to TopHat (especially for INDELS) and other DNA aligners (e. g. bowtie and bwa). The two-pass mode was used to get better alignments around novel splice junctions. The reference genome was that of *Z. marina* which was chosen due to the completeness of gene annotation and relevant information of the sequencing reads (Olsen *et al.*, 2016).

After creating alignment files (BAM), some of the alignments spanning introns were reformatted. By default, this step reassigns mapping qualities for good alignments to match DNA conventions. Mark duplicates, adding Reading group of the Illumina platform and NsplitCigar tools were assessed using the Picard program (Ebbert et al., 2016).

Subsequently, the program GATK was used for variant calling and hard filtering of the data (Liu et al., 2012). Following GATK best-practices on RNA-sequencing, a total number of almost 5000 high quality filtered SNPs was revealed.

Using the program Tassel (Bradbury et al., 2007) the sites were filtered using the filterAlign plugin, where only SNPs that have been scored up to 80% of the individuals were kept. Also, ambiguous sites were discarded. The latter resulted in a total panel of 2036 high quality filtered SNPs.

The parameter used to assess the activity of the photosynthetic apparatus as a measure of the proportion of the light absorbed by the chlorophyll associated with PSII that is used in photochemistry, hence, of plant fitness, was the effective quantum yield (ΔF/Fm'). ΔF/Fm' (Fm' − F'/Fm') was estimated by a diving PAM fluorometer (Walz, Germany), measured at the beginning of the sampling days. The samples were taken from the exposure conditions and directly transferred to a Haake cryothermostat (regulated to experimental temperatures; ±0.2 °C), where ΔF/Fm' was measured. ΔF/Fm' was performed at a standard position on the second leaf approximately 2 cm from the plant meristem (Papathanasiou et al., 2015; Ralph, 2000). The part of the leaf that was sampled for measuring ΔF/Fm' (about 2 cm) was cut at the end of each experiment and stored at −75 °C until leaf Chl-*a* content analysis (Granger and Lizumi, 2001).

In order to determine the type of interaction (additive, synergistic or antagonism) for HOS treatments of *C. nodosa* for the response variables used (ΔF/Fm', leaf Chl-*a* content), the Observed (Obs) effect sizes were compared with the Expected (Exp) additive interaction. The effect sizes were calculated per sampling day per response variable. The Expected effect sizes were calculated based on the sum of effect sizes of each stress, using a multiplicative risk model, which was compared with the Observed combined effect size (Darling et al., 2010). If Obs was greater than the Exp (with no overlap of the 95% Confidence Intervals-CI), then the HOS interaction was classified as synergistic. If Obs was less than the Exp (with no overlap of the 95% CI), then the HOS interaction was classified as antagonistic. If the 95% CI of the Obs overlapped with the 95% CI of the Exp, the HOS interaction was classified as additive.

2.3. Statistical analyses

All analyses were conducted using the R Environment (R Core Team, 2020). Statistical significance between different salinity and temperature conditions as well as the effect of time on each of the previous parameters was determined by an Analysis of Variance (ANOVA) model for each of the 20 heavy metals examined. Differences between 5 levels of Salinity (20, 35, 50, 65, 70) after 6 h of exposure were explored. The effect of Temperature was examined after 6 h at 3 levels: 34, 36, 38 °C, as well as after 1 h at 2 levels – 38 and 40 °C - respectively. The statistically significant effect of time (4 levels: 1, 2, 4, 6 h) was examined at 70 salinity (4 levels: 1, 2, 4, 6 h) and temperature 38 °C (5 levels: 0.5, 1, 2, 4, 6 h), while the effect of both Time (2 levels: 2 and 6 h) and Salinity (2 levels: 65 and 70‰), was tested using a two way ANOVA. Prior to the analysis, data were checked for normality by plotting the theoretical to sample quantiles and by using the shapiro.test() function. When normality was not achieved the function bestNormalize() of the same package (Peterson and Cavanaugh, 2020) was used to find the best transformation of the data. The homogeneity of variance was tested by Levine's test and when the test was significant ($p < 0.05$), a more stringent criterion of $\alpha = 0.01$ was applied to avoid Type I errors (Underwood, 1997). After the analysis, the residuals versus fitted plot was examined for patterns and normality of residuals was tested before accepting the results. When necessary, Post Hoc analysis were conducted using the R Core function TukeyHSD(). All plots were drawn using the "ggplot2" package (Wickham, 2016). All mean values in results are presented with the standard error range.

A similar approach was followed to analyze the effect of fixed independent variable (factor) "Temperature" (four levels: 32, 34, 35 and 36 °C) on *C. nodosa* dependent variables ΔF/Fm' and leaf Chl-*a* content and the effects of factors "Treatment" (four levels: C, HS, OS, HOS) and "Time" (five levels: 1, 3, 5, 10, 20 days) on the dependent variables ΔF/Fm' and leaf Chl-*a* content. One-way repeated measures analysis of variance (rmANOVA) was used to analyze the effect of fixed factor "Salinity" (six levels: 20, 30, 35, 50, 55, 60‰) on ΔF/Fm'. A *post-hoc* comparison test (Student Newman - Keuls, SNK; Zar, 1984) was performed when significant differences were found (Supplementary Table S2).

The number and size of the chloroplasts was measured on digitalized TEM micrographs captured as tiff files (n = 30 different cells for control and treatment each). For the transcriptomics analysis, four different GLM analyses were conducted in the Tassel program (Bradbury et al., 2007): (1) All 12 samples used, with samples grouped according to different stress conditions (aka Control, HS, OS, HOS); (2) Control and HS samples; (3) Control and OS samples; (4) Control and HOS samples. The Bonferonni threshold was calculated to be 2.46 x 10^{-5} (0.05/2036). Genetic variants from GLM were further analyzed with the snpEff program, calculating the effects of variants on known genes.

The software Saguaro (Salomonsen et al., 2014; Zamani et al., 2013) was used to obtain the phylogenetic matrix distances. The software combines a Hidden Markov Model (HMM) with a Self-Organizing Map (SOM) in order to characterize local phylogenetic relationships among aligned sequences of all 12 individuals. Saguaro was run for twenty iterations, after which the set of cacti modelling of the entire genome was saturated and identified ten different cacti that could be grouped into two main classes based on their ability to differentiate the taxa. To create compatible distance matrices for phylogenetic analysis the Saguaro2Phylip functionality *execute* was used. The input file was saguaro.cactus. Using the program Phylip, the functionality *execute neighbour* was used to create phylogenetic trees of the 12 samples. For the visualization of the trees the program FigTree v.1.4.3 (Rambaut, 2012) was assessed.

3. Results

3.1. Ionomic responses

3.1.1. Temperature stress

The tissue levels of almost all the elements investigated were influenced in the same way under heat stress, but Li, Mo, Ni, Cd, Cu, Zn, Rb, Se, B and S were highly increased under heat shock conditions (Suppl. Table 3). Heat shock conditions for *C. nodosa* were 40 °C for 1 h and 38 °C for 4–6 h. Increases of Li, Mo, Ni, Cd, Cu, Zn, Rb, Se, B and S levels were statistically significant after treatment at 40 °C for 1 h. On the other hand, Na was statistically decreased at 40 °C for 1 h.

Under conditions of moderate stress (38 °C for 30 min–2 h), an increase in the tissue levels of P, Na, Sr, Cd and K and a decrease of S was found (Suppl. Fig. S1A). Also, S and Zn seems to be decreased at heat stress (after 6 h at 38 °C).

3.2. Salinity stress

Salinity stress has very similar effects on Li, Mo, Cd, Se, Fe, Cu, Rb and Zn levels. All of them are influenced more by the time of the effect rather than the concentration. In conditions of relatively low levels of stress (2–4 h at salinity 65 and 70‰, respectively), there is an increase in the tissue levels of Li/Mo/Cd/Se/Fe/Cu/Rb/Zn. But after 6 h of stress, concentrations of these metals came back to levels observed in the control (Fig. 2; Suppl. Table S3, Suppl. Fig. S1B).

Mn is influenced in a different way. Under conditions of little stress (2–4 h at salinity 50 or 70‰, respectively) it seems that there is a decrease in the quantity of Mn. But after 6 h of stress, tissue concentrations came back to normal levels (Suppl. Table S3, Suppl. Fig. S1B).

S is influenced by increased salinity. There is a very strong increase after 6 h between salinity 65 and 70‰ (Suppl. Table S3, Suppl. Fig. S1B).

K and Na are influenced by the time of the effect and not the intensity. Under conditions of relatively low levels of stress (2–4 h at salinities of 65 or 70‰, respectively), there is an increase in the levels of K/Na. But after 6 h of stress, concentrations of these metals came back to almost normal levels (Suppl. Table S3, Suppl. Fig. S1B).

3.2.1. Transcriptomic responses

Manhattan plots of transcriptomics data (Suppl. Table S4) using generalized linear model (GLM; Suppl. Fig. S2) showed a pattern of

Table 1
The number of segments/regions (>300 bp), the total length of segments/regions and the percent of *C. nodosa* genome assigned per associated cactus for outlier and neutral loci.

2036 SNPs	Number of regions >300 bp	Cumulative length (bp)	Percent
Cactus 2	94	37,942,949	0.19
Cactus 5	93	24,787,188	0.12
Cactus 7	1	38,326	0.0001

outliers for comparisons between different treatments. When all treatments are compared, among the 129 genomic regions showing clusters of outlier single nucleotide polymorphisms (SNPs), 26 SNPs coded for non-synonymous changes, although *p*-values did not pass for multiple-test correction (Bonferonni threshold: 2,46 x 10^{-5}). When the analyses were split by treatment, multiple significant SNPs coding for non-synonymous changes were found; 17 for Heat stress vs Control, 13 for Osmotic stress vs Control and 7 for Heat-Osmotic stress vs Control. Using the program snpEff, these SNPs were annotated to the *Zostera marina* reference genome and the functional effects of these genetic variants were predicted (Suppl. Table S4).

Above all, an outstanding mutation occurred for osmotic stress, revealing a stop codon at position 745 (p.Arg745*). This genetic region belongs to the RNA exosome, an important protein complex.

In the output file distance matrices are calculated per segment and distance matrices are calculated per cactus (Suppl. Fig. S3). In the present study, the Saguaro program identified 280 segments. For sufficient statistical power, segments of >300 bp were used.

The *Zostera marina* genome length is 203,913,826 bp. Based upon this, the >300 bp cacti assigned to *C. nodosa* and their percentage distribution is presented in Table 1. Thus, the percentage of the genome coverage for Cactus2 and Cactus 4 was 0.31%.

In order to create compatible distance matrices for phylogenetic analysis, the program Saguaro2Phylip was used, while the visualization of the phylogenetic trees was obtained with the program FigTree v.1.4.3. The majority of the transcriptome exhibits neutral genetic divergence (as exemplified by cactus 2), while one cactus (cactus 7), which accounts for 0.0001% of the transcriptome, displays HOS and OS samples clustering (Suppl. Fig. S2).
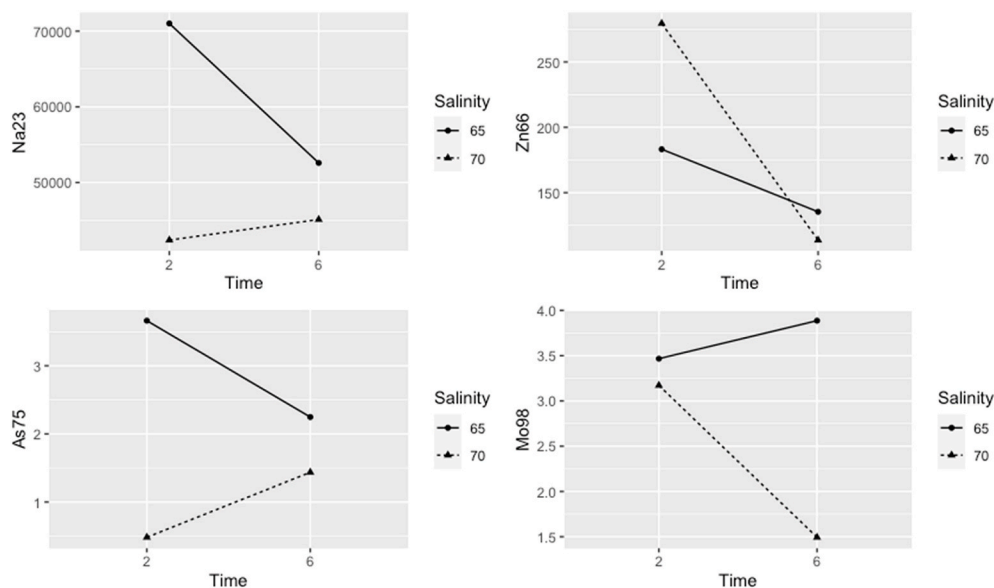

Fig. 2. Variation of tissue metal concentration under two salinity regimes (65 and 70) after 2 and 6 h exposure on four heavy metals, respectively. These were the heavy metals that had statistically significant differences according to two-way ANOVA (Table S2c).

3.3. Non-synonymous changes

A number of non-synonymous changes were revealed through GLM analyses for the different treatment conditions. However, non-significant values (after correction for multiple tests - adjusted p-value: 2.46 x 10^{-5}) were reported when samples were combined altogether. On the other hand, significant associations were found for all other, i.e. three group correlations: 17 for Heat stress vs Control, 13 for Osmotic stress vs Controls and 7 for Heat-Osmotic stress vs Controls. Using the software snpEff, these SNPs were annotated to the *Zostera marina* reference genome (Olsen et al., 2016) and the effects of these genetic variants were predicted (Suppl. Table S4). Overall, most of the non-synonymous changes were associated with metabolic processes (e. g. glutamate catabolism, N-acetylglucosamine metabolism, purine nucleoside catabolism, glucose metabolism) related to enzymatic activity. However, an important non-synonymous change related to metabolism observed during Heat stress treatment is the oxoglutarate dehydrogenase metabolic activity, in which the acetyl group of acetyl coenzyme A is oxidized to two CO_2 and four pairs of electrons are transferred to coenzymes. Moreover, under Heat stress treatment, a non-synonymous change related to the Calmodulin protein could be detected. Calmodulin exerts cellular regulatory activity, which results in the assembly, arrangement of constituent parts, or disassembly of cytoskeletal structures comprising microtubules and their associated proteins (Gaudet et al., 2011). Furthermore, the DNA mismatch repair protein mutS was associated with Heat stress treatment. This protein is associated with cell DNA repair mechanisms such is the correction of the mismatch during meiosis (Paques and Haber, 1999).

As for the Osmotic stress treatment, an outstanding mutation occurred that revealed a stop codon at position 745 (p.Arg745*). This genetic region belongs to the RNA exosome, a protein complex that operates in the breakdown of ribosomal RNA. This genetic region belongs to the RNA exosome, an important complex protein.

In the third group (combined Heat-Osmotic stress treatment), an important non-synonymous change was associated with the Histidine kinase protein, which catalyzes phosphorylation of a histidine residue in response to detection of an extracellular signal such as a chemical ligand or change in environment, to initiate a change in cell state or activity (Gruhn and Heyl, 2013). In addition, this signal triggers a response series of molecular signals generated by the binding of a cytokinin to a receptor, and ending with regulation of a downstream cellular process, e.g. transcription (Cheung and Hendrickson, 2010; Loomis et al., 1997; Stock et al., 2000).

In the output file distance matrices are calculated per segment and distance matrices are calculated per cactus. In the present study, the Saguaro program identified 280 segments. For sufficient statistical power, segments of >300 bp were used.

The *Zostera marina* genome length is 203,913,826 bp. Based upon this, the >300 bp cacti assigned to *Cymodocea nodosa* and their percentage distribution is presented in Table 1. Thus, the percentage of the genome coverage for Cactus2 and Cactus 4 was 0.31%.

In order to create compatible distance matrices for phylogenetic analysis, the program Saguaro2Phylip was used, while the visualization of the phylogenetic trees was obtained with the program FigTree v.1.4.3.
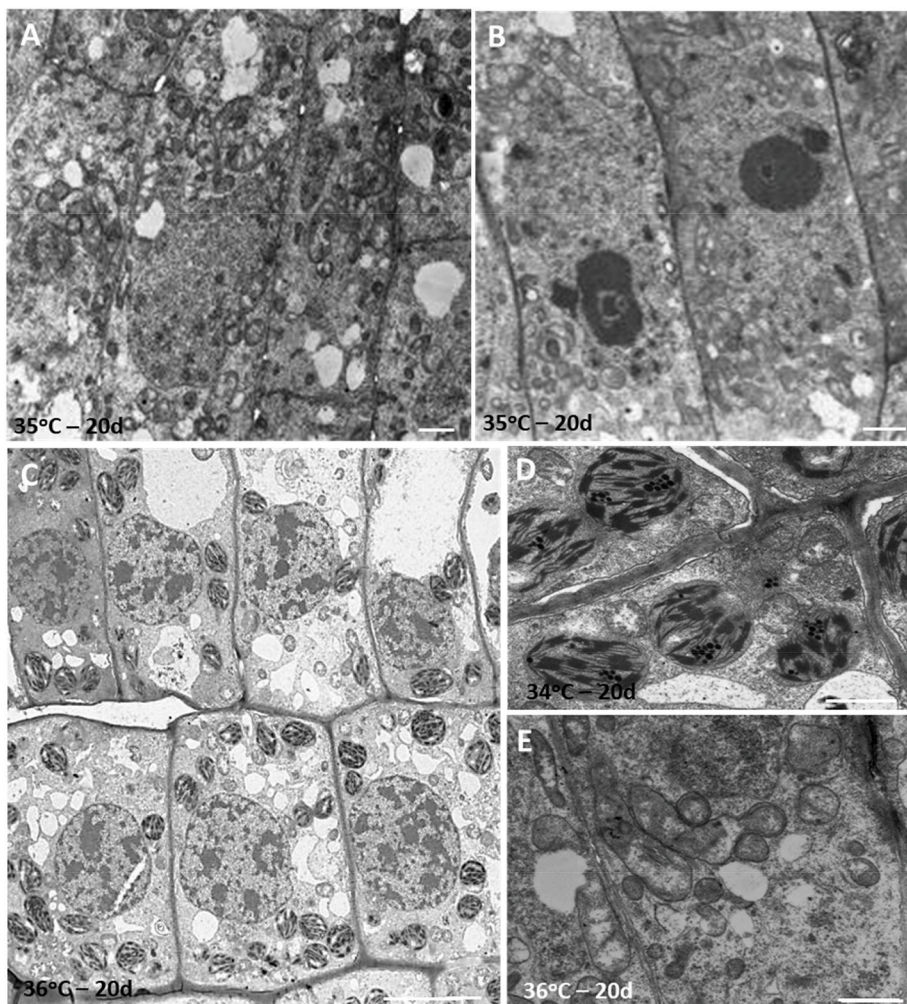

Fig. 3. TEM micrographs of young leaf cells of *C. nodosa* in heat stressed material. **A.** Epidermal cells in paradermal leaf section. **B.** Higher magnification of nucleus with the appearance of an electron transparent ring inside the nucleoli. **C.** Epidermal cells with condensed masses of chromatin within the nuclei. **D.** Disorganized chloroplasts with few thylakoid bands. **E.** Lobe-shaped mitochondria with membrane protrusions and disorganized cristae. Scale bars = 1 μm (A, B, C) and 0.3 μm (D, E), respectively.

3.4. Cell structure and MT organization

3.4.1. Temperature stress

Incubation at 32 °C for 20 days did not cause serious disturbance in cell structure. Chloroplasts were increased in number and their thylakoid and grana organization was typical. On the contrary, incubation at 34 °C, 35 °C and 36 °C for 20 days, respectively, caused severe changes in cell structure. The nucleus is losing its typical oval shape and attaining an amoeboid – like shape (Fig. 3A, C). Nuclei showed condensed masses of chromatin (Fig. 3C) and in some interphase cells, nucleoli were characterized by the presence of an electron transparent ring (Fig. 3B). Chloroplasts also presented rather unusual morphology. Their shape was round (Fig. 3D) and their number appeared increased, almost double, compared to the control. Plastoglobuli were also increased in the chloroplasts. Mitochondria were numerous, with aberrant shape, including broken and sometimes dilated cristae (Fig. 3E).

Microtubule cytoskeleton was also investigated in leaf cells after incubation at 32, 34 and 36 °C, for 20 days. MTs of interface cells were drastically affected, appearing as short bundles of varying thickness and random orientations (Fig. 5A, C). In some cells spots of tubulin polymers were observed (Fig. 5C). In particular, aberrant orientation of MT bundles was found at 32 °C (Fig. 5A and B), as well as star-like or helical configurations at 34 °C (Fig. 5C), or ring-like MT configurations at 36 °C (Fig. 5D and E). In addition, dividing cells appeared also affected by heat stress. The number of dividing cells was lower compared to the control, and cells with preprophase MT band were not found. Cells which were dividing at the beginning of the treatment were blocked and mitotic spindles appeared consisting of thick and short MT bundles.

3.4.2. Salinity stress

Incubation at high salinities of 50‰ for 20 days caused changes in cell structure (Fig. 4A). The cells were highly vacuolated with large vacuoles (Fig. 4A). Masses of condensed chromatin inside the nucleus were present (Fig. 4B). Chloroplasts also were bigger in size with limited numbers of thylakoids and undifferentiated grana (Fig. 4C). Based on counting 30 cells from the control material and 30 cells from the material exposed to salinity stress (data not shown), their number was around 30% higher than that of the control cells. Mitochondria were numerous, with aberrant shape, including broken and sometimes dilated cristae.

Incubation at low salinities of 20‰ for 20 days caused changes in cell wall structure (Fig. 4D). The cell walls were very thick (Fig. 4D). There was an increase of the proportion of oval-shaped chloroplasts with well-organized grana and thylakoids (Fig. 4E). Based on counting 30 cells
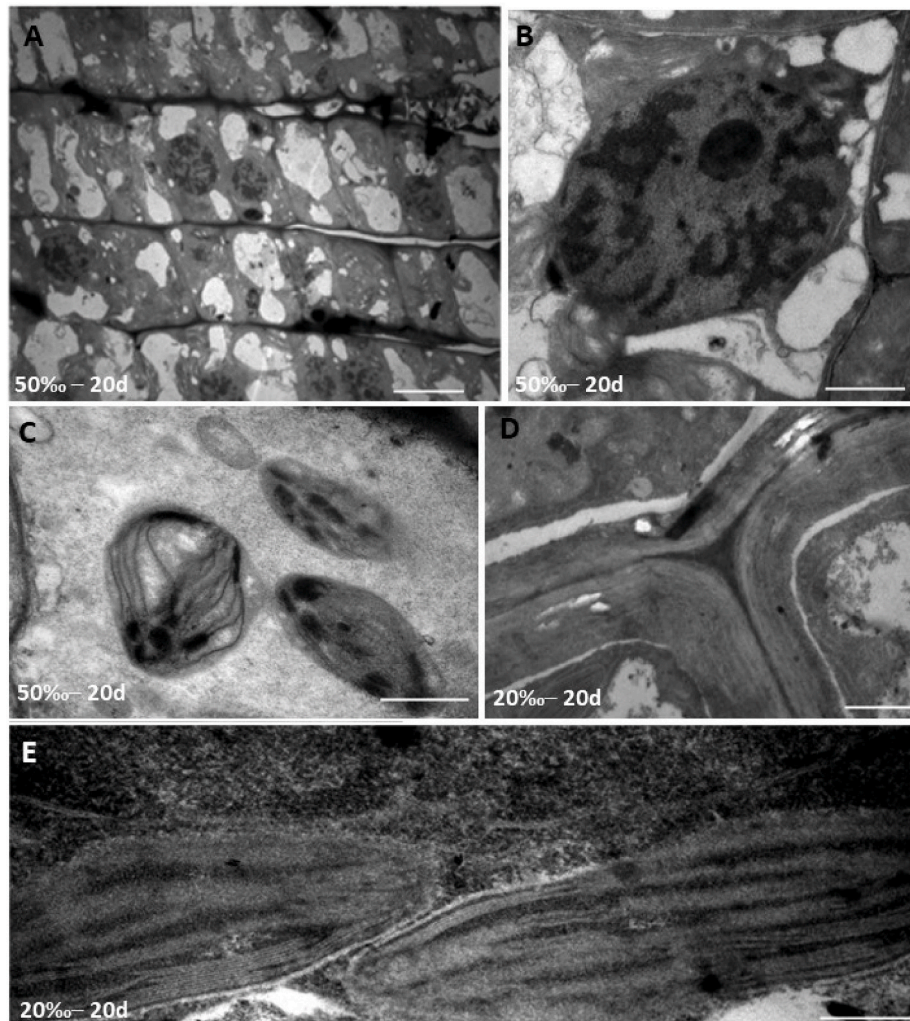

Fig. 4. TEM micrographs of young leaf cells of *C. nodosa* in high and low salinity stressed material **A.** Epidermal, highly vacuolated cells in paradermal leaf section in salinity stressed material. **B.** Nucleus with condensed masses of chromatin **C.** Well-sized chloroplasts. **D.** Thick cell wall in low salinity **E.** Well sized chloroplasts with thylakoids and grana. Scale bars= 1 μm (A) and 0.3 μm (B, C, D, E), respectively.
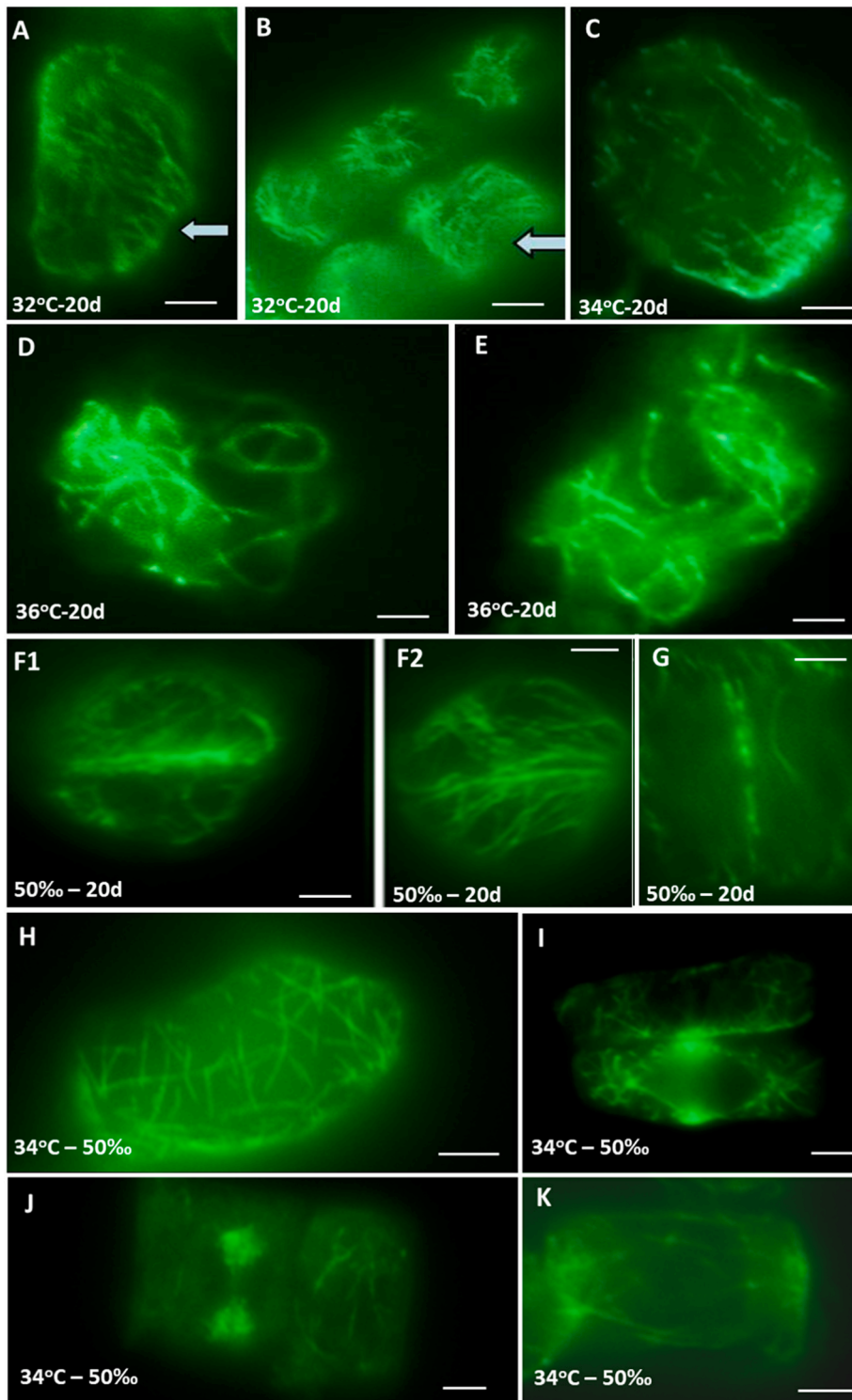
Fig. 5. Immunofluorescence images of interphase epidermal cells of young leaves of *C. nodosa* **i.** under heat stress **A.** Thin, fragmented, slightly misoriented MT bundles **B.** Mt bundles, forming a helical-like configuration **C.** Incubation at 34 °C for 20 days: MT bundles with aberrant orientations **D-E.** Incubation at 36 °C: short and thick MT bundles with aberrant orientations, wavy in shape, forming ring-like configurations. **ii.** under salinity stress salinity 50 for 20 days **F-G.** Telophase - cytokinetic cell with abnormal phragmoplast. **iii.** under heat and salinity stress 34 °C - salinity 50 for 20 days **H.** Thin fragmented MT bundles with loss of orientation. **I-K.** Prophase cell with abnormal mitotic spindle **J.** Telophase cell with normal phragmoplast with parallel MTs bundles. Scale bars = 10 μm.

from the control material and 30 cells from the material exposed to salinity stress (data not shown), their size was around 40% bigger than that of the control cells. Also, fibrillar and granular zones around the nucleoli were segregated and the shape of mitochondria was changed to lobe-shaped with protrusions.

Microtubule cytoskeleton was also investigated after salinity treatment at 50‰ and 20‰ for 20 days. In high salinities MTs of interface cells appeared as short, thin bundles with random orientation (Fig. 5F). Some of them appeared fragmented with spots of tubulin polymers at the

sites of newly synthesized cell walls (Fig. 5F and G). In low salinities appeared normal parallel bundles oriented perpendicularly to the long leaf axis.

3.4.3. Combined salinity and temperature stress

The effects of treatment in the HS and OS groups for 20 days were the same as described above (temperature stress and salinity stress respectively). HOS experiments showed that typical MT organization was disturbed. Short and/or thick MT bundles were observed, together with

Table 2
A. One-way analysis of variance (ANOVA) summary table used to analyze the effect of fixed independent variable (factor) "Temperature" (four levels: 32, 34, 35 and 36 °C) on *C. nodosa* dependent variables ΔF/Fm' and leaf Chl-*a* content. **B.** One-way repeated measures ANOVA for ΔF/Fm' and one-way ANOVA of leaf Chl-*a* content of *C. nodosa* with salinity (20, 30, 35, 50, 55 and 60‰, respectively). **C.** Two-way analysis of variance (ANOVA) summary table used to analyze the effects of factors "Treatment" (four levels: C, HS, OS, HOS) and "Time" (five levels: 1, 3, 5, 10, 20 days) on the dependent variables ΔF/Fm' and leaf Chl-*a* content.

A. Thermal stress		D.F.	MS	F	*p*
ΔF/Fm'	Intercept	1	11.32	564.97	0.00
	Temperature (°C)	3	0.02	0.95	0.44
	Error	19	0.02		
Chl-*a*	Intercept	1	695.25	431.22	0.00
	Temperature (°C)	3	29.41	18.24	0.00
	Error	19	1.61		
B. Salinity stress					
ΔF/Fm'	Intercept	1	106.67	5066.86	<0.001
	Salinity	5	0.34	16.03	<0.001
	Error	29	0.02		
	Time*Salinity	6	0.09	27.90	<0.001
	Time*Salinity	30	0.02	5.13	<0.001
	Error	174	0.00		
Chl-*a*	Intercept	1	216.62	206.93	<0.001
	Salinity	5	8.73	8.34	<0.001
	Error	29	1.05		
C. Interaction of stresses		D.F.	MS	F	*p*
ΔF/Fm'	Intercept	1	61.33	48614.82	0.00
	Day	4	0.00	3.82	0.01
	Treatment	3	0.04	33.32	0.00
	Day*Treatment	12	0.00	0.66	0.78
	Error	98	0.00		
Chl-*a*	Intercept	1	853.87	741.64	0.00
	Day	4	11.54	10.02	0.00
	Treatment	3	14.76	12.82	0.00
	Day*Treatment	12	5.80	5.04	0.00
	Error	100	1.15		

MTs with aberrant orientations (Fig. 5H). Cells with preprophase band were not found and mitotic spindles appeared affected, consisting of thick and short MT bundles (Fig. 5I, K). However, the phragmoplast appeared normal (Fig. 5J).

3.5. Photosynthetic and leaf Chl-*a* content responses

3.5.1. Temperature stress
No statistically significant difference was observed along the upper temperatures tested on ΔF/Fm' ($p > 0.05$, Table 2A). The highest mean value of ΔF/Fm' of *C. nodosa* was measured at 32 °C (0.753 ± 0.03) while lowest at 36 °C (0.623 ± 0.232) (Fig. 6). The effect of temperature on leaf Chl-*a* content was statistically significant ($p < 0.001$, Table 2A). *C. nodosa* had the highest leaf Chl-*a* content at 34 °C (7.83 ± 0.7 mg/g) and the lowest at 36 °C (2.63 ± 1.12 mg/g) (Fig. 6). *Post-hoc* comparisons indicated that leaf Chl-*a* content at 36 °C was statistically different from all other treatments (Suppl. Table S2).

3.5.2. Salinity stress
The effect of salinity on ΔF/Fm' of *C. nodosa* was statistically significant ($p < 0.001$, Table 2B). The highest mean ΔF/Fm' was observed at a salinity of 30‰ (0.734 ± 0.01), while the minimum was observed at 60‰ (0.51 ± 0.0) (Fig. 7). The effect of salinity on leaf Chl-*a* content was statistically significant ($p < 0.001$, Table 2B). *Cymodocea nodosa* had the highest leaf Chl-*a* content at salinity 35‰ (3.96 ± 0.6 mg/g), while the lowest was observed at 60‰ (0.98 ± 0.09 mg/g) (Fig. 7). *Post-hoc* comparisons indicated that leaf Chl-*a* content at salinities of 50, 55 and 60‰, respectively, were statistically lower than after all other

treatments (Suppl. Table S2).

3.5.3. Combined salinity and temperature stress
The effects of treatment ($p < 0.001$) and time ($p < 0.01$) on ΔF/Fm' were statistically significant (Table 2C). Highest mean ΔF/Fm' was measured at Days 10 and 20 of HS group (0.78 ± 0.005 and 0.768 ± 0.002, respectively) and the lowest at Days 3 and 1 of OS group (0.649 ± 0.02 and 0.651 ± 0.03, respectively; Fig. 8). *Post-hoc* comparisons showed that OS and HS groups were statistically different from all other treatments. The interaction of treatment and time was statistically significant on leaf Chl-*a* content ($p < 0.001$). Highest leaf Chl-*a* content was measured at day 10 of HS group (5.99 ± 0.34 mg/g) and lowest at day 1 of OS group (1.16 ± 0.21 mg/g; Fig. 8). *Post-hoc* comparisons showed that the HS group differed statistically from all other groups and on Day 10, the HS group was significantly different from all the other treatments (Suppl. Table S2).

3.5.4. Interaction types
The interaction types for the HOS treatment per sampling day for the response variables -ΔF/Fm' and leaf Chl-*a* content-are shown in Fig. 9. The HOS interaction for ΔF/Fm' was found to be additive (with strong antagonistic trend) on the 1st day, additive on the 3rd day, additive (with strong antagonistic trend) on the 5th and 10th day and antagonistic on the 20th day. The HOS interaction for the leaf Chl-*a* content was additive (with antagonistic trend) on the 1st day, additive on the 3rd, 5th and 10th day and additive (with synergistic trend) on the 20th day. In the majority of the cases examined, OS effect size was greater that the HS effect size, showing that salinity stress affected the response variables more that the heat stress.

4. Discussion

Taken together, the multi-disciplinary approach of this study shows that both high temperature and salinity, alone and in combination, respectively, affected the physiology and cell biology of *C. nodosa* at multiple levels. Overall, it is obvious that salt stress had a greater impact on *C. nodosa* (Table 3) than heat stress both at an ionomic, transcriptomic, ultrastructural and physiological level. Indeed, salt stress is one of the major environmental stresses limiting photosynthesis (Sudhir and Murthy, 2004) and plant growth (Isayenkov and Maathuis, 2019). This is the first study applying large-scale ionomics to a seagrass. A recent study (Garrote-Moreno et al., 2016) explored the concentrations of 4 ions in 4 seagrass species experimentally exposed to hypo- and hyperosmotic stress, respectively.

4.1. Molecular evolution for permanent underwater life

During their evolution towards an overall adaptation to the marine environment, seagrasses had to develop specific molecular, physiological and morphological adaptations (Olsen et al., 2016; Wissler et al., 2011). The evolutionary implications of differential transcriptome genotypes of osmotic stress which affect the ecophysiology of *C. nodosa* were established in this study by detecting non-synonymous changes, which may alter the ecology of the species under certain environmental conditions, Supporting the strategy of a given species for colonization and adaptation to habitats suited to its genotype (Exadactylos, 2015; Malandrakis et al., 2017b). Such intraspecific diversity which is possible due to phenotypic plasticity could lead to rapid speciation in a challenging environment. Gkafas et al. (2016) reported a significant diversity of the species in question among different geographical areas, also when correlating with topographic and oceanographic features. The reported non-synonymous changes may be due to a primary phylogenetic division, such as illustrated with Saguaro analysis. Thus, the habitat may lead to divisions in population dynamics suggesting conspecific ecotypes associated with high osmotic levels. This independent assessment of genomic regions associated with osmosis (cacti

Table 3

Overview of results.

Treatment	Tubulin Immunofluorescence – Microtubule organization	Electron microscopy - Cell structure	Leaf Chl-a content	Photosynthetic performance – ΔF/Fm'
30°C – 3 weeks	Same as control	Normally sized vacuoles occupy a significant part of the cell space; limited number of thylakoids and developing grana (30% decrease)		
32°C – 3 weeks	Parallel bundles oriented perpendicularly to the long leaf axis/ slight disturbance of MTs (5% were misoriented)	Number of chloroplasts increased (20%)	Optimum mean Chl-*a* content	Optimum mean ΔF/Fm' values
34°C – 3 weeks	Short fragmented MT bundles, loss of orientation/phragmoplast with disordered MTs/short fragmented MTs at the preprophase zone	Normally-sized vacuoles occupy a significant part of the cell space; number of chloroplasts was increased (20%); shape of mitochondria was changed – lobe-shaped with protrusions and disorganized cristae; chloroplasts with round plastoglobuli	Highest mean value, statistically significantly higher than the concentration observed at 35 and 36 °C, respectively	Optimum mean ΔF/Fm' values
35–36°C – 3 weeks	Thick, fragmented MTs bundles with loss of their orientation forming cycles/nucleus has not elliptical shape and structure	Increase of the proportion of oval-shaped chloroplasts (30%) with limited number of thylakoids and developing grana and greater number of round plastoglobuli; nucleus with loose and partially disrupted nuclear membrane with fibrillar and granular zones around the nucleoli; shape of mitochondria was changed to lobe-shaped with protrusions and disorganized cristae	At 36 °C lowest Chl-*a* content was observed, significantly lower than at 35 °C (which is also low in comparison to the whole series)	Plants at 35 °C had slightly lower mean ΔF/Fm' values than the plants subject to other treatments; plants at 36 °C had lowest mean ΔF/Fm' values in comparison to the whole series
20‰ – 3 weeks	Parallel bundles oriented perpendicularly to the long leaf axis	Increase of the proportion of oval-shaped chloroplasts (40%) with well-organized grana and thylakoids; very thick cell walls; fibrillar and granular zones around the nucleoli were segregated; the shape of mitochondria was changed to lobe-shaped with protrusions	Plants at 20‰ had higher Chl-*a* content than plants at 55‰	Optimum mean ΔF/Fm' values
50‰ – 3 weeks	Short fragmented MT bundles; loss of orientation; phragmoplast with disordered MTs; short fragmented MTs at the preprophase zone	Highly vacuolated cells; increase of oval-shaped chloroplasts (30%) with limited number of thylakoids and developing grana; mitochondria with disorganized cristae	Plants at 50‰ had significantly higher Chl-*a* content than plants at 55‰, while plants at 55‰ had the statistically lowest Chl-*a* content that the whole series	Plants at 55‰ had the significantly lowest mean ΔF/Fm' values in comparison to the whole series; Plants at 50‰ had optimum mean ΔF/Fm' values

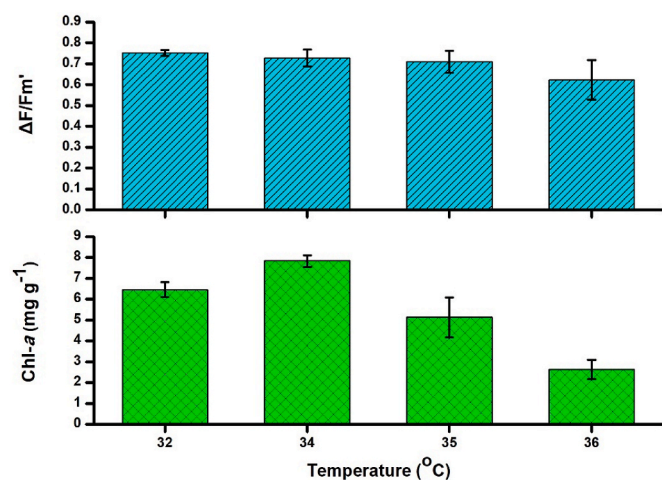**Fig. 6.** Mean values of effective quantum yield (ΔF/Fm') and leaf Chl-*a* content (±SE, n = 6) of *C. nodosa* after 20 days of treatment at 32, 34, 35 and 36 °C.

Fig. 7. Mean values of effective quantum yield (ΔF/Fm') and leaf Chl-*a* content (±SE, n = 6) of *C. nodosa* after 20 days of treatment at salinities 20, 30, 35, 50, 55 and 60.

plots; Supplementary Fig. S2) reinforced the evidence for selection. These strong genomic associations suggest considerable species adaptation to specific environmental stress.
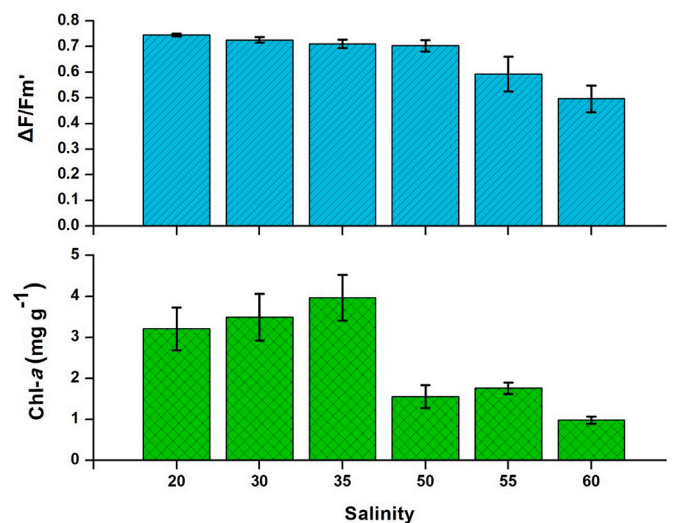
4.2. Interactive salinity and temperature effects

During heat events in the Mediterranean Sea, especially around noon, the relatively high air temperatures cause high evaporation,
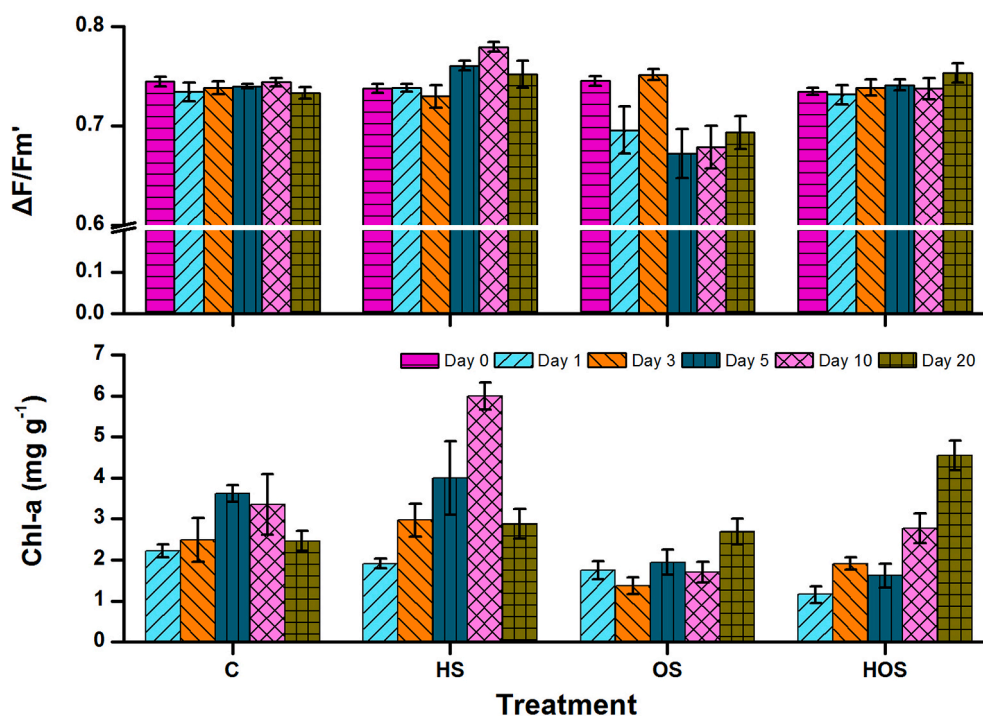
Fig. 8. Mean values of effective quantum yield (ΔF/Fm') and leaf Chl-*a* content (±SE, n = 6) of *C. nodosa* on 0, 1, 3, 5, 10 and 20 sampling days for each treatment. C = Control, HS = Heat Stress, OS = Osmotic Stress, HOS = Heat and Osmotic Stress.

resulting in a high salinity in shallow coastal waters, where the seagrasses and *C. nodosa* thrives. Similar conditions of increased temperature and salinities in the range of those which are applied in this study are likely to occur is that of brine discharge near seawater desalination plants which have been found to impact seagrass meadows (Fernandez-Torquemada and Sanchez-Lizaso, 2005; Latorre, 2005; Xevgenos et al., 2021) including the species studied here (Garrote-Moreno et al., 2014).

Seagrasses have developed various physiological strategies to overcome the detrimental effects of high salinity, such as diffusion from the cytoplasmic compartment into the chloroplasts, leading to a decreased efficiency of photosynthesis (Sudhir and Murthy, 2004).

Under high salinity plants use less photon energy for photosynthesis with the excess of energy to decline the effective quantum yield and damage of PSII, if the dissipation per active reaction centers is not efficient enough (Duarte et al., 2013; Qiu et al., 2003). Also, photosynthetic carbon capture is affected by disturbances on leaf water relations and osmotic potential, on the chloroplast membrane systems and on the chlorophyll pigment composition (Munns, 1993).

Cymodocea nodosa tolerated and showed optimum responses of photosynthetic performance (ΔF/Fm') and leaf Chl-*a* content at salinities between 10 and 50 (Fernandez-Torquemada and Sanchez-Lizaso, 2005; Pagès et al., 2010; Tsioli et al., 2019). During hypersaline stress, *C. nodosa* activates osmoregulatory mechanisms involving soluble sugars (Sandoval-Gil et al., 2014), cell-wall-hardening processes (Sandoval-Gil et al., 2012), and ion-exclusion mechanisms (Garrote-Moreno et al., 2015).

Remarkably, the data from the combined 50‰ salinity and 34 °C temperature treatments (HOS) indicated an antagonistic interaction on ΔF/Fm'. Therefore, higher energy supply was due to a better balance between the formation of excited states of chlorophyll *a* in PSII following light absorption by PSII, and the dissipation of these excited states of chlorophyll-*a* photochemically (Genty et al., 1989). It is noteworthy that, since stress is dose-dependent, in this study, we chose comparable values of salinity (50‰) and temperature (34 °C) with both leading the

treated plants to the stage of the resistance response phase (Tsioli et al., 2019), following the stress definition of Lichtenthaler (1996a) as any unfavourable condition or substance that affects or blocks the metabolism, growth or development of a plant. In agreement, Ontoria et al. (2020) also found out that the response of the seagrass *Halophila ovalis* under a combined short-term salinity increase and a transient temperature stress had a positive effect on Gross P_{max}. This suggests that increased salinities might dampen the adverse effects of high temperatures, thus buffering, to some extent, the impact of marine heatwaves in the context of climate change.

Different studies provide clear evidence for extreme differences in stressor interactions within a single species, ranging from additive to antagonism and synergism across a range of possible factors, such as duration of stress (Crain et al., 2008; Darling and Côté, 2008). For example, under interaction of HOS for ΔF/Fm' was additive with a solid antagonistic trend at the beginning and antagonistic at the end of the experiment. The HOS interaction for the leaf Chl-*a* content was additive with an antagonistic trend and ended as additive with a synergistic trend.

Salinity stress is also considered as a hyperionic stress (Gupta and Huang, 2014). One of the most detrimental effects of salinity stress is the accumulation of Na^+ and Cl^- ions in tissues of plants exposed to high NaCl concentrations. Entry of both Na^+ and Cl^- into the cells causes severe ion imbalance and excess uptake might cause significant physiological disorder(s). High Na^+ concentrations inhibit uptake of K^+ ions which is an essential element for growth and development that results into lower productivity and may even lead to death (Marschner, 2011; Wilson and Dunton, 2018). K is abundant in the cytoplasm and plays a role in osmoregulation with implications for cell extension and growth. It helps establish the electrochemical gradient across membranes. Interactions that links Fe with Mn include reactive oxygen species (ROS). Furthermore, Fe in combination with Zn, might be involved in various transporters. Mg plays a role in ATPases and in ribosome subunits and in biosynthesis of the chlorophyll molecule. In this study, the Na and K concentrations were influenced by the time of treatment: after 6 h of
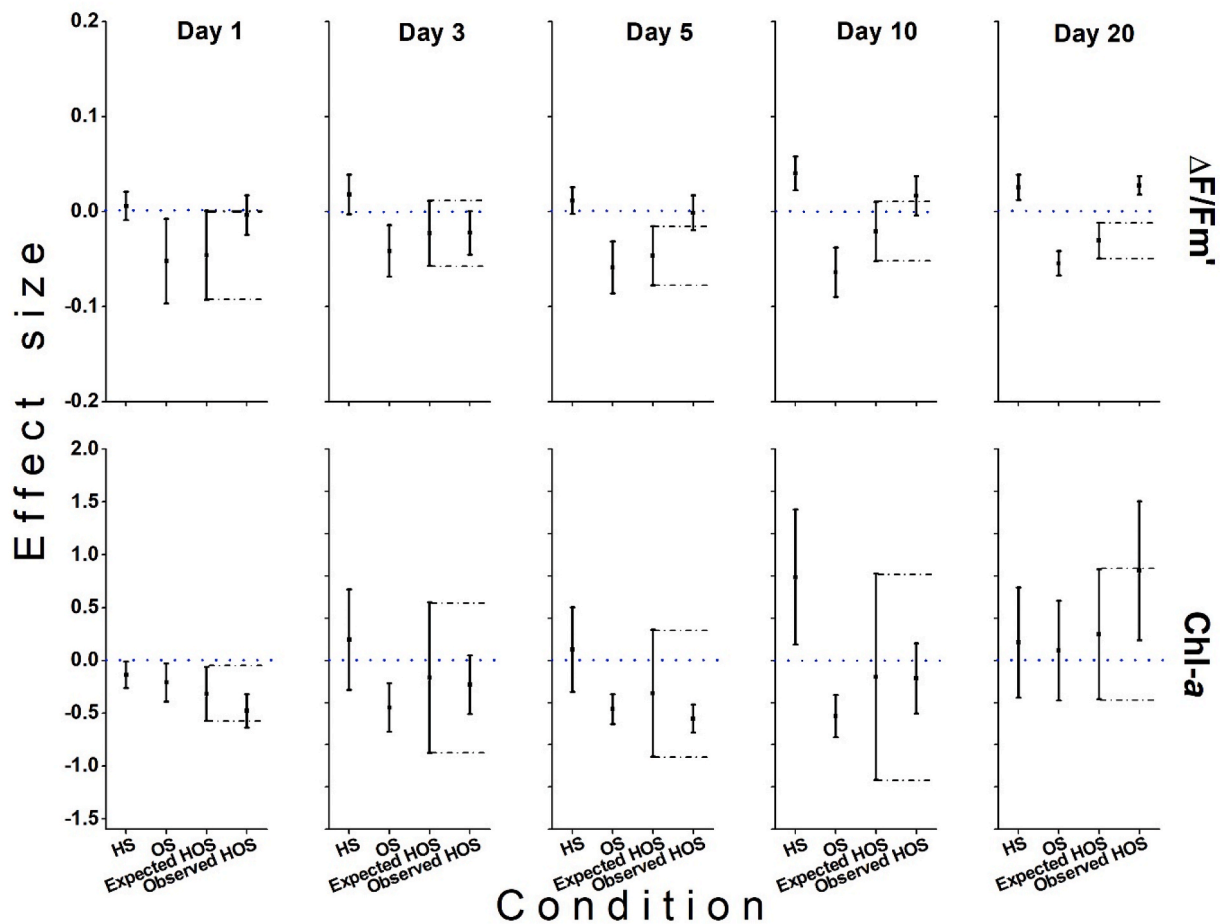
Fig. 9. Effect sizes (± 95% CI) per treatment day for effective quantum yield (ΔF/Fm') and leaf Chl-*a* content (mg g^{-1}) of *C. nodosa* under heat stress (HS, salinity 35 - temperature 34 °C), osmotic stress (OS, salinity 35 - temperature 22 °C), the Expected additive and Observed of the combined heat and osmotic stress (HOS; salinity 50‰ - temperature 34 °C).

stress, concentrations of these metals came back to almost normal levels. Obviously, the duration and intensity of stress used in this study was not too high to allow the metabolism of *Cymodocea* a degree of regulation of such ions.

Under heat and salinity stress, the cellular and cytoskeleton disturbances incurred elicit mechanisms in order to protect cells from damage that stress may cause. Cultivation for 20 d at 34, 35 and 36 °C as well as 50 salinity caused visible alterations in the structure of cell organelles. The nucleolus formed electron dense granules or an electron transparent ring which maybe caused from the pre-rRNA synthesis (Fransolet et al., 1979). Also, the DNA fragmentation could be related with programmed cell death (PCD; Reape and McCabe, 2008). The increased number of mitochondria under stress conditions could be linked with the increasing demand for ATP production which is caused when photosynthesis is damaged (Silva et al., 2010). This could also be linked with the increased demand for mitochondrial stress proteins (Rizhsky et al., 2002, 2004). In conclusion, temperatures above 34 °C and salinities of 50‰ or higher result in severe perturbations in cytoskeleton organization, meaning that the MT cytoskeleton is a sensitive indicator of stress conditions under abiotic stress in seagrasses (Koutalianou et al., 2016; Malea et al., 2013a, b).

Moreover, the differences observed at transcriptomic level under osmotic stress vs. control relate mostly to elongation factors and protein kinases which are related to cell structure and development – these expression differences were associated with alterations in cell structure (larger chloroplasts, lower levels of Chl-*a* and ΔF/Fm', and fragmented

MTs in the cytoskeleton). The latter support the special strategy of the species for colonization and adaptation to habitats suited to their genotype.

Regarding high temperatures, it is well known that photosynthesis is affected by thermal stress which has harmful effects up to death, since photosystems and the electron transport system are heat-sensitive (Collier and Waycott, 2014; Repolho et al., 2017). The effects of heat stress include chronic PSII damage (Collier and Waycott, 2014) and potential cellular damage and cytoskeleton disturbances (Koutalianou et al., 2016). Thermal stress typically increases the fluidity of thylakoid membranes and PSII light-harvesting complexes fall off the thylakoid membranes, which results in impaired PSII integrity and affects photosynthetic electron transfer (Mathur et al., 2014). The oxygen evolving complex (OEC) in PSII is dissociated by heat stress, which further results in the inhibition of electron transport from the OEC to the acceptor side of PSII (Strasser et al., 2004). Therefore, only species with a high degree of physiological plasticity can cope with abrupt changes, such as heat waves (Duarte et al., 2018). Marín-Guirao et al. (2016) stated that *C. nodosa* can inhabit shallow environments with high thermal stress, due to its ability to maintain elevated photosynthetic electron flow and to sustain enhanced photosynthesis during heat exposure. Indeed, while mean ΔF/Fm' values of *C. nodosa* were the highest at 32 °C (0.753), at 36 °C was lower (0.623) but not statistical significantly (Fig. 8). In addition, the maximum leaf Chl-*a* content observed at 34 °C indicates the plant's high potential for acclimation under the heat stress.

Overall, this study showed that all levels of biological hierarchy

Table 4
Overview of conclusions.

DISCUSSION	Tubulin Immunofluorescence - Microtubule organization	Electron microscopy - Cell structure	Ionomics	Leaf Chl-*a* content	Photosynthetic ability	Molecular results
HS - Heat stress	Disturbance in shape, density and orientation of MTs; MT network was atypically organized with loss of transverse orientation and presence of thick, fragmented MT bundles; dividing cells were blocked at telophase cytokinesis	The cellular damages and cytoskeleton disturbances elicit cellular stress responses (CSR) in order to protect cells from damage that heat stress may cause; the CSR can increase the tolerance and remove already damaged cells through **apoptosis**	Deficiencies of P, K, S impact metabolites involved in photosynthesis and respiration. This leads to inadequancies in the transfer of light energy to chemical bonds or in the export of sugars from chloroplasts and result in the development of **necrotic** leaves. Similar deficiencies of Zn, Mn can impair ezyme activity or the function of structural proteins and overall metabolism is reduced	**Highest** Chl-*a* content was observed at HS/ Day 10, significantly higher from all other treatments.	HS plants had the **highest** mean ΔF/Fm' values was observed at days 10 & 20	Plant **chloroplasts** express the *matK* gene that is required for the splicing of essential plastid tRNAs and rRNAs. Also it plays a role under cadmium stress and zinc stress. *AHP4* belongs to the Hpt family the key signal sensing machinery which enables organisms **sense** and respond to **external stimulus**/activation of heat responsive transcription factors/ influenced of genes encoding **photosynthetic** proteins
OS - Osmotic stress	Short fragmented MT bundles loss of orientation/ phragmoplast normal/short fragmented MTs at the preprophase band	Highly vacuoled cells and disturbance of chloroplasts shows no significant damages/ osmoregulation mechanisms for cell **homeostasis**	K is abundant in cytoplasm and plays role in **osmoregulation,** affects cell extension and growth. It helps establish the electrochemical gradient across membranes/Interactions that links Fe with Mn might be reactive oxygen species **ROS,** also Fe with Zn might be various **transporters**/Mg plays role in ATPases and in ribosome subunits and in porphyrin (chlorophyl molecule)	**Normal** Chl-*a* content was observed at OS during the experimental period	OS plants had the **lowest** mean ΔF/Fm' values in comparison to the whole series during the experimental period; The OS effect size was greater than the HS effect size, in most of the cases	*RLK1* is involved in salt stress signal transduction and enhances plant **tolerance** to high salinity/organic solutes accumulated in cytoplasm in order to counteract the osmotic potential of **accumulated ions in the vacuole**

investigated were strongly affected by applied temperature and salinity stress, however, with the latter having more severe effects (Table 4). This may be correlated with the evolution of the species in question from terrestrial to marine life.

Author contributions

All authors contributed to experiments and lab work. GAA and AE conducted bioinformatics. AE, SO and CIK obtained the finding and directed this project strategically and day-to-day, with guidance from FCK. FCK led the writing of this article, supported by all authors.

Data availability statement

The data supporting the findings of this study are available from the corresponding author, Frithjof C. Küpper, upon request.

Author statement

Soultana Tsioli: Conceptualization, Methodology, Investigation, Writing – Original Draft, Review & Editing, Visualization. Maria Koutalianou: Conceptualization, Methodology, Investigation, Writing – Original Draft, Review & Editing, Visualization. Georgios A. Gkafas: Conceptualization, Methodology, Investigation, Formal Analysis, Data Curation, Writing – Original Draft, Review & Editing, Visualization. Athanasios Exadactylos: Conceptualization, Methodology, Writing – Original Draft, Review & Editing, Project Administration, Funding Acquisition. Vasilis Papathanasiou: Conceptualization, Methodology, Investigation, Formal Analysis, Writing – Original Draft, Review & Editing, Visualization. Christos I. Katsaros: Conceptualization, Methodology, Writing – Original Draft, Review & Editing, Visualization, Supervision, Project Administration, Funding Acquisition. Sotiris Orfanidis: Conceptualization, Methodology, Investigation, Formal Analysis, Writing – Original Draft, Review & Editing, Visualization, Supervision, Project Administration, Funding Acquisition. Frithjof C. Küpper: Conceptualization, Methodology, Formal Analysis, Writing – Original Draft, Review & Editing, Supervision, Visualization, Project Administration.

Declaration of competing interest

The authors declare that they have no known competing financial interests or personal relationships that could have appeared to influence the work reported in this paper.

Appendix A. Supplementary data

Supplementary data to this article can be found online at https://doi.org/10.1016/j.marenvres.2021.105512.

References

Benjamin, K.J., Walker, D.I., McComb, A.J., Kuo, J., 1999. Structural response of marine and estuarine plants of *Halophila ovalis* (R. Br.) Hook. f. to long-term hyposalinity. Aquat. Bot. 64, 1–17.

Bradbury, P.J., Zhang, Z., Kroon, D.E., Casstevens, T.M., Ramdoss, Y., Buckler, E.S., 2007. TASSEL: software for association mapping of complex traits in diverse samples. Bioinformatics 23, 2633–2635.

Cancemi, G., Buia, M.C., Mazzella, L., 2002. Structure and growth dynamics of *Cymodocea nodosa* meadows. Sci. Mar. 66, 365–373.

Cheung, J., Hendrickson, W.A., 2010. Sensor domains of two-component regulatory systems. Curr. Opin. Microbiol. 13, 116–123.

Collier, C.J., Waycott, M., 2014. Temperature extremes reduce seagrass growth and induce mortality. Mar. Pollut. Bull. 83, 483–490.

Crain, C.M., Kroeker, K., Halpern, B.S., 2008. Interactive and cumulative effects of multiple human stressors in marine systems. Ecol. Lett. 11, 1304–1315.

Danku, J.M.C., Gumaelius, L., Baxter, I., Salt, D.E., 2009. A high-throughput method for *Saccharomyces cerevisiae* (yeast) ionomics. J. Anal. At. Spectrom. 24, 103–107.

Darling, E.S., Côté, I.M., 2008. Quantifying the evidence for ecological synergies. Ecol. Lett. 11, 1278–1286.

Darling, E.S., McClanahan, T.R., Côté, I.M., 2010. Combined effects of two stressors on Kenyan coral reefs are additive or antagonistic, not synergistic. Conservation Letters 3, 122–130.

De Pascalis, F., Perez-Ruzafa, A., Gilabert, J., Marcos, C., Umgiesser, G., 2012. Climate change response of the Mar Menor coastal lagoon (Spain) using a hydrodynamic finite element model. Estuar. Coast Shelf Sci. 114, 118–129.

Den-Hartog, C., 1970. The Seagrasses of the World. North Holland Publications, Amsterdam.

Dobin, A., Davis, C.A., Schlesinger, F., Drenkow, J., Zaleski, C., Jha, S., Batut, P., Chaisson, M., Gingeras, T.R., 2013. STAR: ultrafast universal RNA-seq aligner. Bioinformatics 29, 15–21.

Dobin, A., Gingeras, T.R., 2015. Mapping RNA-seq Reads with STAR. Curr. Protoc. Bioinf. 51, 11.14.1–11.14.19.

Duarte, B., Martins, I., Rosa, R., Matos, A.R., Roleda, M.Y., Reusch, T.B.H., Engelen, A.H., Serrão, E.A., Pearson, G.A., Marques, J.C., Caçador, I., Duarte, C.M., Jueterbock, A., 2018. Climate change impacts on seagrass meadows and macroalgal forests: an integrative perspective on acclimation and adaptation potential. Front. Mar. Sci. 5.

Duarte, B., Santos, D., Marques, J.C., Caçador, I., 2013. Ecophysiological adaptations of two halophytes to salt stress: photosynthesis, PS II photochemistry and anti-oxidant feedback – implications for resilience in climate change. Plant Physiol. Biochem. 67, 178–188.

Ebbert, M.T.W., Wadsworth, M.E., Staley, L.A., Hoyt, K.L., Pickett, B., Miller, J., Duce, J., Kauwe, J.S.K., Ridge, P.G., for the Alzheimer's Disease Neuroimaging, Initiative, 2016. Evaluating the necessity of PCR duplicate removal from next-generation sequencing data and a comparison of approaches. BMC Bioinf. 17, 239.

Ermgassen, P.S.E., Grabowski, J.H., Gair, J.R., Powers, S.P., 2016. Quantifying fish and mobile invertebrate production from a threatened nursery habitat. J. Appl. Ecol. 53, 596–606.

Exadactylos, A., 2015. Molecular approach of seagrasses response related to tolerance acquisition to abiotic stress. In: Caliskan, M., Oz, G.C., Kavakli, I.H., Ozcan, B. (Eds.), Molecular Approaches to Genetic Diversity. IntechOpen, London.

Fernandez-Torquemada, Y., Sanchez-Lizaso, J.L., 2005. Effects of salinity on leaf growth and survival of the Mediterranean seagrass *Posidonia oceanica* (L.) Delile. J. Exp. Mar. Biol. Ecol. 320, 57–63.

Fernandez-Torquemada, Y., Sanchez-Lizaso, J.L., 2011. Responses of two Mediterranean seagrasses to experimental changes in salinity. Hydrobiologia 669, 21–33.

Fransolet, S., Deltour, R., Bronchart, R., Van de Walle, C., 1979. Changes in ultrastructure and transcription induced by elevated temperature in *Zea mays* embryonic root cells. Planta 146, 7–18.

Galli, G., Solidoro, C., Lovato, T., 2017. Marine heat waves hazard 3d maps and the risk for low motility organisms in a warming mediterranean sea. Front. Mar. Sci. 4.

Garrote-Moreno, A., Cambridge, M., Sanchez-Lizaso, J.L., 2016. Ion concentrations in seagrass: a comparison of results from field and controlled-environment studies. Estuar. Coast Shelf Sci. 181, 209–217.

Garrote-Moreno, A., Fernandez-Torquemada, Y., Sanchez-Lizaso, J.L., 2014. Salinity fluctuation of the brine discharge affects growth and survival of the seagrass *Cymodocea nodosa*. Mar. Pollut. Bull. 81, 61–68.

Garrote-Moreno, A., Sandoval-Gil, J.M., Ruiz, J.M., Marín-Guirao, L., Bernardeau-Esteller, J., Muñoz, R.G., Sánchez-Lizaso, J.L., 2015. Plant water relations and ion homoeostasis of Mediterranean seagrasses (*Posidonia oceanica* and *Cymodocea nodosa*) in response to hypersaline stress. Mar. Biol. 162, 55–68.

Gaudet, P., Livstone, M.S., Lewis, S.E., Thomas, P.D., 2011. Phylogenetic-based propagation of functional annotations within the Gene Ontology consortium. Briefings Bioinf. 12, 449–462.

Genty, B., Briantais, J.-M., Baker, N.R., 1989. The relationship between the quantum yield of photosynthetic electron transport and quenching of chlorophyll fluorescence. Biochim. Biophys. Acta Gen. Subj. 990, 87–92.

Gerakaris, V., Lardi, P.L., Issaris, Y., 2020. First record of the tropical seagrass species *Halophila decipiens* Ostenfeld in the Mediterranean Sea. Aquat. Bot. 160.

Gkfas, G., Orfanidis, S., Vafidis, D., Panagiotaki, P., Kuepper, F., Exadactylos, A., 2016. Genetic diversity and structure of *Cymodocea nodosa* meadows in the aegean sea, eastern meditterranean. Appl. Ecol. Environ. Res. 14, 145–160.

Golicz, A.A., Schliep, M., Lee, H.T., Larkum, A.W.D., Dolferus, R., Batley, J., Chan, C.-K. K., Sablok, G., Ralph, P.J., Edwards, D., 2015. Genome-wide survey of the seagrass *Zostera muelleri* suggests modification of the ethylene signalling network. J. Exp. Bot. 66, 1489–1498.

Granger, S.Granger, Lizumi, H., 2001. Water quality measurement methods for seagrass habitat. In: Short, F.T., Coles, R.G., Short, C.A. (Eds.), Global seagrass research methods. Elsevier Science: Amsterdam., pp. 393–406. ISBN 0-444-50891-0. VII, 473 pp.

Gruhn, N., Heyl, A., 2013. Updates on the model and the evolution of cytokinin signaling. Curr. Opin. Plant Biol. 16, 569–574.

Gupta, B., Huang, B., 2014. Mechanism of salinity tolerance in plants: physiological, biochemical, and molecular characterization. Int. J. Genom. 2014, 701596.

He, Q., 2019. Climate change, human impacts, and coastal ecosystems in the Anthropocene. Curr. Biol. 29, R1021–R1035.

Hobday, A.J., Alexander, L.V., Perkins, S.E., Smale, D.A., Straub, S.C., Oliver, E.C.J., Benthuysen, J.A., Burrows, M.T., Donat, M.G., Feng, M., Holbrook, N.J., Moore, P.J., Scannell, H.A., Sen Gupta, A., Wernberg, T., 2016. A hierarchical approach to defining marine heatwaves. Prog. Oceanogr. 141, 227–238.

Hoegh-Guldberg, O., Mumby, P.J., Hooten, A.J., Steneck, R.S., Greenfield, P., Gomez, E., Harvell, C.D., Sale, P.F., Edwards, A.J., Caldeira, K., Knowlton, N., Eakin, C.M., Iglesias-Prieto, R., Muthiga, N., Bradbury, R.H., Dubi, A., Hatziolos, M.E., 2007. Coral reefs under rapid climate change and ocean acidification. Science 318, 1737–1742.

Humanes, A., Noonan, S.H.C., Willis, B.L., Fabricius, K.E., Negri, A.P., 2016. Cumulative effects of nutrient enrichment and elevated temperature compromise the early life history stages of the Coral *Acropora tenuis*. PLoS One 11, e0161616.

Isayenkov, S.V., Maathuis, F.J.M., 2019. Plant salinity stress: many unanswered questions remain. Front. Plant Sci. 10.

Iyer, V., Barnabas, A.D., 1993. Effects of varying salinity on leaves of *Zostera capensis* Setchell. I. Ultrastructural changes. Aquat. Bot. 46, 141–153.

Jagels, R., Barnabas, A., 1989. Variation in leaf ultrastructure of *Ruppia maritima* L. along a salinity gradient. Aquat. Bot. 33, 207–221.

Katsaros, C., Galatis, B., 1992. Immunofluorescence and electron-microscopic studies of microtubule organization during the cell-cycle of *Dictyota dichotoma* (Phaeophyta, Dictyotales). Protoplasma 169, 75–84.

Katsaros, C., Galatis, B., Mitrakos, K., 1983. Fine-structural studies on the interphase and dividing apical cells of *Sphacelaria tribuloides* (Phaeophyta). J. Phycol. 19, 16–30.

Koch, M.S., Schopmeyer, S.A., Kyhn-Hansen, C., Madden, C.J., Peters, J.S., 2007. Tropical seagrass species tolerance to hypersalinity stress. Aquat. Bot. 86, 14–24.

Koutalianou, M., Orfanidis, S., Katsaros, C., 2016. Effects of high temperature on the ultrastructure and microtubule organization of interphase and dividing cells of the seagrass *Cymodocea nodosa*. Protoplasma 253, 299–310.

Küpper, F.C., Kamenos, N.A., 2018. The future of marine biodiversity and marine ecosystem functioning in UK coastal and territorial waters (including UK Overseas Territories) – with an emphasis on marine macrophyte communities. Bot. Mar. 61, 521–535.

Lahner, B., Gong, J.M., Mahmoudian, M., Smith, E.L., Abid, K.B., Rogers, E.E., Guerinot, M.L., Harper, J.F., Ward, J.M., McIntyre, L., Schroeder, J.I., Salt, D.E., 2003. Genomic scale profiling of nutrient and trace elements in *Arabidopsis thaliana*. Nat. Biotechnol. 21, 1215–1221.

Lamit, N., Tanaka, Y., 2021. Effects of river water inflow on the growth, photosynthesis, and respiration of the tropical seagrass *Halophila ovalis*. Bot. Mar. 64, 93–100.

Latorre, M., 2005. Environmental impact of brine disposal on *Posidonia* seagrasses. Desalination 182, 517–524.

Lichtenthaler, H.K., 1996a. Vegetation stress: an introduction to the stress concept in plants. J. Plant Physiol. 148, 4–14.

Lichtenthaler, H.K., 1996b. Vegetation stress: an introduction to the stress concept in plants. J. Plant Physiol. 148, 4–14.

Liu, Q., Guo, Y., Li, J., Long, J.R., Zhang, B., Shyr, Y., 2012. Steps to ensure accuracy in genotype and SNP calling from Illumina sequencing data. BMC Genom. 13, S8.

Loomis, W.F., Shaulsky, G., Wang, N., 1997. Histidine kinases in signal transduction pathways of eukaryotes. J. Cell Sci. 110, 1141–1145.

Malandrakis, E.E., Dadali, O., Kavouras, M., Danis, T., Panagiotaki, P., Miliou, H., Tsioli, S., Orfanidis, S., Küpper, F.C., Exadactylos, A., 2017a. Identification of the abiotic stress-related transcription in little Neptune grass *Cymodocea nodosa* with RNA-seq. Marine Genomics 34, 47–56.

Malandrakis, E.E., Danis, T., Iona, A., Exadactylos, A., 2017b. Abiotic stress of seagrasses: recent advances in transcriptomics, genomics, and systems biology. In: Kumar, M.,

Ralph, P. (Eds.), Systems Biology of Marine Ecosystems. Springer International Publishing, Cham, pp. 119–132.

Malea, P., Adamakis, I.D.S., Kevrekidis, T., 2013a. Kinetics of cadmium accumulation and its effects on microtubule integrity and cell viability in the seagrass *Cymodocea nodosa*. Aquat. Toxicol. 144, 257–264.

Malea, P., Adamakis, I.D.S., Kevrekidis, T., 2013b. Microtubule integrity and cell viability under metal (Cu, Ni and Cr) stress in the seagrass *Cymodocea nodosa*. Chemosphere 93, 1035–1042.

Marbà, N., Duarte, C.M., 2010. Mediterranean warming triggers seagrass (*Posidonia oceanica*) shoot mortality. Global Change Biol. 16, 2366–2375.

Marín-Guirao, L., Ruiz, J.M., Dattolo, E., Garcia-Munoz, R., Procaccini, G., 2016. Physiological and molecular evidence of differential short-term heat tolerance in Mediterranean seagrasses. Sci. Rep. 6, 28615.

Marschner, H., 2011. Marschner's Mineral Nutrition of Higher Plants. Academic press.

Mathur, S., Agrawal, D., Jajoo, A., 2014. Photosynthesis: response to high temperature stress. J. Photochem. Photobiol. B Biol. 137, 116–126.

Maxwell, K., Johnson, G.N., 2000. Chlorophyll fluorescence—a practical guide. J. Exp. Bot. 51, 659–668.

McKenna, A., Hanna, M., Banks, E., Sivachenko, A., Cibulskis, K., Kernytsky, A., Garimella, K., Altshuler, D., Gabriel, S., Daly, M., DePristo, M.A., 2010. The Genome Analysis Toolkit: a MapReduce framework for analyzing next-generation DNA sequencing data. Genome Res. 20, 1297–1303.

Munns, 1993. Physiological processes limiting plant growth in saline soils: some dogmas and hypotheses. Plant Cell Environ. 16, 15–24.

Olsen, J.L., Rouze, P., Verhelst, B., Lin, Y.C., Bayer, T., Collen, J., Dattolo, E., De Paoli, E., Dittami, S., Maumus, F., Michel, G., Kersting, A., Lauritano, C., Lohaus, R., Topel, M., Tonon, T., Vanneste, K., Amirebrahimi, M., Brakel, J., Bostrom, C., Chovatia, M., Grimwood, J., Jenkins, J.W., Jueterbock, A., Mraz, A., Stam, W.T., Tice, H., Bornberg-Bauer, E., Green, P.J., Pearson, G.A., Procaccini, G., Duarte, C.M., Schmutz, J., Reusch, T.B.H., Van de Peer, Y., 2016. The genome of the seagrass *Zostera marina* reveals angiosperm adaptation to the sea. Nature 530, 331–335.

Ontoria, Y., Webster, C., Said, N., Ruiz, J.M., Pérez, M., Romero, J., McMahon, K., 2020. Positive effects of high salinity can buffer the negative effects of experimental warming on functional traits of the seagrass *Halophila ovalis*. Mar. Pollut. Bull. 158, 111404.

Orfanidis, S., Panayotidis, P., Stamatis, N., 2001. Ecological evaluation of transitional and coastal waters: a marine benthic macrophytes-based model. Mediterr. Mar. Sci. 2/2, 45–65.

Orfanidis, S., Papathanasiou, V., Gounaris, S., Theodosiou, T., 2010. Size distribution approaches for monitoring and conservation of coastal *Cymodocea* habitats. Aquat. Conserv. Mar. Freshw. Ecosyst. 20, 177–188.

Pagès, J.F., Pérez, M., Romero, J., 2010. Sensitivity of the seagrass *Cymodocea nodosa* to hypersaline conditions: a microcosm approach. J. Exp. Mar. Biol. Ecol. 386, 34–38.

Pandey, P., Irulappan, V., Bagavathiannan, M.V., Senthil-Kumar, M., 2017. Impact of combined abiotic and biotic stresses on plant growth and avenues for crop improvement by exploiting physio-morphological traits. Front. Plant Sci. 8.

Papathanasiou, V., Orfanidis, S., 2018. Anthropogenic eutrophication affects the body size of *Cymodocea nodosa* in the North Aegean Sea: a long-term, scale-based approach. Mar. Pollut. Bull. 134, 38–48.

Papathanasiou, V., Orfanidis, S., Brown, M.T., 2015. Intra-specific responses of *Cymodocea nodosa* to macro-nutrient, irradiance and copper exposure. J. Exp. Mar. Biol. Ecol. 469, 113–122.

Paques, F., Haber, J.E., 1999. Multiple pathways of recombination induced by double-strand breaks in *Saccharomyces cerevisiae*. Microbiol. Mol. Biol. Rev. 63, 349.

Pergent, G., Bazairi, H., Bianchi, C.N., Boudouresque, C., Buia, M., Calvo, S., Clabaut, P., HarmelinVivien, M., Angel Mateo, M., Montefalcone, M., 2014. Climate Change and Mediterranean Seagrass Meadows: a Synopsis for Environmental Managers.

Peterson, R.A., Cavanaugh, J.E., 2020. Ordered quantile normalization: a semiparametric transformation built for the cross-validation era. J. Appl. Stat. 47, 2312–2327.

Qiu, N., Lu, Q., Lu, C., 2003. Photosynthesis, photosystem II efficiency and the xanthophyll cycle in the salt-adapted halophyte *Atriplex centralasiatica*. New Phytol. 159, 479–486.

R Core Team, 2020. R: A language and environment for statistical computing. R Foundation for Statistical Computing, Vienna, Austria.

Ralph, P.J., 2000. Herbicide toxicity of Halophila ovalis assessed by chlorophyll a fluorescence. Aquat. Bot. 66, 141–152.

FigTree, version 1.4.3 Rambaut, A., 2012, Computer program distributed by the author, website. http://tree.bio.ed.ac.uk/software/figtree/ [accessed January 4, 2011.

Reape, T.J., McCabe, P.F., 2008. Apoptotic-like programmed cell death in plants. New Phytol. 180, 13–26.

Repolho, T., Duarte, B., Dionísio, G., Paula, J.R., Lopes, A.R., Rosa, I.C., Grilo, T.F., Caçador, I., Calado, R., Rosa, R., 2017. Seagrass ecophysiological performance under ocean warming and acidification. Sci. Rep. 7, 41443.

Rizhsky, L., Liang, H.J., Mittler, R., 2002. The combined effect of drought stress and heat shock on gene expression in tobacco. Plant Physiol. 130, 1143–1151.

Rizhsky, L., Liang, H.J., Shuman, J., Shulaev, V., Davletova, S., Mittler, R., 2004. When Defense pathways collide. The response of *Arabidopsis* to a combination of drought and heat stress. Plant Physiol. 134, 1683–1696.

Salomonsen, J., Chattaway, J.A., Chan, A.C.Y., Parker, A., Huguet, S., Marston, D.A., Rogers, S.L., Wu, Z., Smith, A.L., Staines, K., Butter, C., Riegert, P., Vainio, O., Nielsen, L., Kaspers, B., Griffin, D.K., Yang, F., Zoorob, R., Guillemot, F., Auffray, C.,

Beck, S., Skjødt, K., Kaufman, J., 2014. Sequence of a complete chicken BG haplotype shows dynamic expansion and contraction of two gene lineages with particular expression patterns. PLoS Genet. 10, e1004417.

Salt, D.E., Baxter, I., Lahner, B., 2008. Ionomics and the study of the plant ionome. Annu. Rev. Plant Biol. 59, 709–733.

Sandoval-Gil, J.M., Marín-Guirao, L., Ruiz, J.M., 2012. The effect of salinity increase on the photosynthesis, growth and survival of the Mediterranean seagrass *Cymodocea nodosa*. Estuar. Coast Shelf Sci. 115, 260–271.

Sandoval-Gil, J.M., Ruiz, J.M., Marín-Guirao, L., Bernardeau-Esteller, J., Sánchez-Lizaso, J.L., 2014. Ecophysiological plasticity of shallow and deep populations of the Mediterranean seagrasses *Posidonia oceanica* and *Cymodocea nodosa* in response to hypersaline stress. Mar. Environ. Res. 95, 39–61.

Serra, T.S., Figueiredo, D.D., Cordeiro, A.M., Almeida, D.M., Lourenço, T., Abreu, I.A., Sebastián, A., Fernandes, L., Contreras-Moreira, B., Oliveira, M.M., Saibo, N.J.M., 2013. OsRMC, a negative regulator of salt stress response in rice, is regulated by two AP2/ERF transcription factors. Plant Mol. Biol. 82, 439–455.

Sghaier, Y.R., Zakhama-Sraieb, R., Benamer, I., Charfi-Cheikhrouha, F., 2011. Occurrence of the seagrass *Halophila stipulacea* (hydrocharitaceae) in the southern Mediterranean sea. Bot. Mar. 54, 575–582.

Silva, E.N., Ferreira-Silva, S.L., Fontenele, A.D., Ribeiro, R.V., Viegas, R.A., Silveira, J.A. G., 2010. Photosynthetic changes and protective mechanisms against oxidative damage subjected to isolated and combined drought and heat stresses in *Jatropha curcas* plants. J. Plant Physiol. 167, 1157–1164.

Smale, D.A., Wernberg, T., Oliver, E.C.J., Thomsen, M., Harvey, B.P., Straub, S.C., Burrows, M.T., Alexander, L.V., Benthuysen, J.A., Donat, M.G., Feng, M., Hobday, A. J., Holbrook, N.J., Perkins-Kirkpatrick, S.E., Scannell, H.A., Sen Gupta, A., Payne, B. L., Moore, P.J., 2019. Marine heatwaves threaten global biodiversity and the provision of ecosystem services. Nat. Clim. Change 9, 306–312.

Stock, A.M., Robinson, V.L., Goudreau, P.N., 2000. Two-component signal transduction. Annu. Rev. Biochem. 69, 183–215.

Stockbridge, J., Jones, A.R., Gillanders, B.M., 2020. A meta-analysis of multiple stressors on seagrasses in the context of marine spatial cumulative impacts assessment. Sci. Rep. 10, 11934.

Strasser, R.J., Tsimilli-Michael, M., Srivastava, A., 2004. Analysis of the chlorophyll a fluorescence transient. In: Papageorgiou, G.C., Govindjee (Eds.), Chlorophyll a Fluorescence: A Signature of Photosynthesis. Springer Netherlands, Dordrecht, pp. 321–362.

Sudhir, P., Murthy, S., 2004. Effects of salt stress on basic processes of photosynthesis. Photosynthetica 42, 481–486.

Trevathan-Tackett, S.M., Kelleway, J., Macreadie, P.I., Beardall, J., Ralph, P., Bellgrove, A., 2015. Comparison of marine macrophytes for their contributions to blue carbon sequestration. Ecology 96, 3043–3057.

Tsioli, S., Orfanidis, S., Papathanasiou, V., Katsaros, C., Exadactylos, A., 2019. Effects of salinity and temperature on the performance of *Cymodocea nodosa* and *Ruppia cirrhosa*: a medium-term laboratory study. Bot. Mar. 62, 97–108.

Tsioli, S., Papathanasiou, V., Rizouli, A., Kosmidou, M., Katsaros, C., Papastergiadou, E., Küpper, F.C., Orfanidis, S., 2021. Diversity and Composition of Algal Epiphytes on the Mediterranean Seagrass *Cymodocea Nodosa*: a Scale-Based Study. Bot. Mar. (in press).

Underwood, A.J., 1997. Experiments in Ecology: Their Logical Design and Interpretation Using Analysis of Variance. University of Sydney, Sydney.

Waycott, M., Procaccini, G., Les, D.H., Reusch, T.B.H., 2006. Seagrass Evolution, Ecology and Conservation: A Genetic Perspective, Seagrasses: Biology, Ecology and Conservation. Springer Netherlands, Dordrecht, pp. 25–50.

Wernberg, T., Smale, D.A., Thomsen, M.S., 2012. A decade of climate change experiments on marine organisms: procedures, patterns and problems. Global Change Biol. 18, 1491–1498.

Wickham, H., 2016. ggplot2: Elegant Graphics for Data Analysis. Springer, New York.

Wilson, S.S., Dunton, K.H., 2018. Hypersalinity during regional drought drives mass mortality of the seagrass *Syringodium filiforme* in a subtropical lagoon. Estuar. Coast 41, 855–865.

Wissler, L., Codoñer, F.M., Gu, J., Reusch, T.B., Olsen, J.L., Procaccini, G., Bornberg-Bauer, E., 2011. Back to the sea twice: identifying candidate plant genes for molecular evolution to marine life. BMC Evol. Biol. 11, 1–13.

Xevgenos, D., Marcou, M., Louca, V., Avramidi, E., Ioannou, G., Argyrou, M., Stavrou, P., Mortou, M., Küpper, F.C., 2021. Aspects of environmental impacts of seawater desalination: Cyprus as a case study. Desalin. Water Treat. 211, 15–30.

Yamamoto, Y., 2016. Quality control of Photosystem II: the mechanisms for avoidance and tolerance of light and heat stresses are closely linked to membrane fluidity of the thylakoids. Front. Plant Sci. 7, 1136.

York, P.H., Gruber, R.K., Hill, R., Ralph, P.J., Booth, D.J., Macreadie, P.I., 2013. Physiological and morphological responses of the temperate seagrass *Zostera muelleri* to multiple stressors: investigating the interactive effects of light and temperature. PLoS One 8, e76377.

Zamani, N., Russell, P., Lantz, H., Hoeppner, M.P., Meadows, J.R.S., Vijay, N., Mauceli, E., di Palma, F., Lindblad-Toh, K., Jern, P., Grabherr, M.G., 2013. Unsupervised genome-wide recognition of local relationship patterns. BMC Genom. 14, 347.

Zhao, G.Q., Ma, B.L., Ren, C.Z., 2007. Growth, gas exchange, chlorophyll fluorescence, and ion content of naked oat in response to salinity. Crop Sci. 47, 123–131.